Sika deer antler as a novel model to investigate dental implant healing

Dissertation
zur Erlangung des Doktorgrades (PhD)
der Medizinischen Fakultät
der Rheinischen Friedrich-Wilhelms-Universität
Bonn

Dr. med. dent. Yun He
aus Yibin/China
2019

Angefertigt mit der Genehmigung
der Medizinischen Fakultät der Universität Bonn

1. Gutachter: Univ.-Prof. Dr. rer. nat. Christoph Bourauel
2. Gutachter: Prof. Dr. med. dent. Friedhelm Heineman
3. Mitglied: Univ.-Prof. Dr. med. dent. Gerhard Wahl
4. Mitglied: Univ.-Prof. Dr. med. dent. Helmut Stark

Tag der Mündlichen Prüfung: 08.02.2019

Aus der Poliklinik für Zahnärztliche Prothetik, Propädeutik
und Werkstoffwissenschaften der Universität Bonn
Direktor: Univ.-Prof. Dr. med. dent. H. Stark
- Stiftungsprofessur für Oralmedizinische Technologie –
Univ.-Prof. Dr. rer. nat. C. Bourauel

Table of Contents

List of Abbreviations

AC	Attenuation coefficient
ANOVA	Analysis of variance
BMD	Bone mineral density
FE	Finite element
IL	Immediate loading
µCT	Micro-computed tomography
PMMA	Polymethylmethacrylate
SD	Standard deviation
SPSS	Statistical Package for the Social Sciences
SNK	Student-Newman-Keuls

1. Abstract

The rapid growth and periodic regeneration of antlers make Sika deer a good and less invasive alternative model for studying bone remodelling. In this study, we developed a special loading protocol for dental implants inserted into deer antlers and analysed the bone reaction around dental implants under immediate loading (IL) and unloaded conditions until and how far osseointegration took place. The aim was to reveal changes in the structure and density of antler tissue during the healing phase, and observe the biomechanical properties of the implant and the surrounding antler tissue. Six healthy 4-year-old male captive bred and tamed Sika deer (Cervus nippon) were utilised in this study. Two implants per antler were inserted. One implant was loaded immediately via a self-developed loading device, the other was submerged and unloaded as control. IL implants were harvested after different loading periods. The unloaded implants were collected after the shedding of antler. Specimens were scanned in a µCT scanner and the density of antler tissue around the implants was measured. Furthermore, samples were fixed, immersed, photopolymerised and parallelly cut in 100 to 200 µm thick sections. After grinding, sections were stained using toluidine blue and evaluated under light microscope. Moreover, finite element (FE) models were generated from the µCT data by using FE software package. A vertical force of 10 N was applied on the implant.

The mean values of maximum displacements, stresses and strains were compared and statistically analysed. The results showed that the density of antler tissue around the implants increased as the loading time increased. This finding was histologically confirmed by the good osseointegration that was observed in unloaded and loaded specimens. Besides, antler tissue displayed a similar healing process to human bone. After shedding the antler, the density of antler tissue remained in a similar value in all specimens. The maximum values of displacements and stresses in the implant and stresses and strains in antler tissue were significantly different among unloaded models and between loaded models. In one antler, all the biomechanical parameters of loaded model were significantly higher than those of unloaded model of the same animal ($P<0.05$) and wider distributions were obtained from loaded model.

It can be concluded that implants inserted into Sika deer antler might not disturb the growth and the calcification process of antler and the use of Sika deer antler model is a promising alternative for implant studies that does not require animal sacrifice.

2. Dissertation Summary

2.1 Introduction

Dental implants are important tools for restoring the loss of single teeth and to support dental prostheses after accidents, diseases or age-related loss of teeth (Abboud et al., 2005). Dental implants improve the quality of a patient's life by improving aesthetics and phonetics and by decreasing the bone resorption processes in the alveolar ridge. In particular, IL dental implants (one-stage technique) are an emerging treatment alternative that may be described as a functional loading immediately after implantation without waiting for a healing period with primary osseointegration (Al-Sawai et al., 2016; Barndt et al., 2015). In contrast, the conventional protocol advocates a two-stage technique with a load-free healing phase for three to six months (Albrektsson et al., 1981; Brånemark, 1983). Apparently, IL implants offer fast dental restoration and pain relief (Abboud et al., 2005; Götz et al., 2010) and provide both physical and psychological benefits to the patients.

Research regarding complex bone remodelling processes occurring around IL dental implants is crucial to improve their function and acceptance. Therefore, *in vivo* models are required, and animal trials have previously been conducted in dogs (Huang et al., 2015; Mainetti et al., 2015; Simion et al., 2015), rabbits (Han et al., 2014; Kunnekel et al., 2011; Vandamme et al., 2007) or rats (Matin et al., 2003; Sato et al., 2014). The results indicated that IL had a positive effect on the tissue differentiation and bone formation around titanium implants, and IL significantly increased bone stress during the early postoperative period. However, these animal experiments are problematic due to different reasons. Firstly, the investigation commonly causes an enormous stress due to repeated anesthetisation and surgery of the animals in order to realise a controlled loading protocol. Secondly, the load applied on endosseous implants is difficult to control, because the loading device in the mouth or on top of other bone sites might be affected by many factors, such as food intake and physiologic activity. Last but not least, the fortune of the animals is sacrifice, which restricted an intensive investigation of bone tissue due to ethical reasons.

Deer are the only mammals that are capable of fully regenerating a complex organ, called antlers (Li et al., 2014). The ability to fully regenerate stands out as the most impressive feature of antlers. Antlers start to grow from bony pedicles placed on the head of male Sika deer in winter or spring and are enveloped in vascularised velvet, the periosteum, during growth (Gaspar-López et al., 2010). The growth rate may reach up to 1.2 cm per day during the 70 days of the fastest growth period (Gaspar-López et al., 2010). In summer, growth ceases and antlers are completely mineralised. In addition, the velvet is shed, thereby exposing the bare bone of the so-called hard antlers from July to August (Gaspar-López et al., 2010; Gomez et al., 2006). The development of an abscission layer across the base induces casting of the antlers to complete the cycle and to enable subsequent regrowth (Currey et al., 2009; Landete-Castillejos et al., 2012; Meng et al., 2015; Szuwart et al., 2002). This allows carrying out investigations of IL dental implants in a relatively acceptable time span without affecting the naturation of the future antlers.

Being sensitive to manipulation during growth, antlers are barely sensitive when growth is completed, as they are intended to be used as weapons to fight against conspecifics. This enables also the implants to be placed over a prolonged time in the antlers as well and to retrieve them when antlers are regularly shed by the deer. Furthermore, deer antlers with high collagen content and the ability to bear tensile and compressive forces in their normal functional state have similar elastic and fracture behaviour to that of human bone (Currey et al., 2009). Besides, as a muscle- and joint-free bony cranial appendage (Kierdorf et al., 2003; Li et al., 2005), antlers provide a fascinating model to investigate the effect of loading on bone remodelling process around IL implants without the influence of external forces (except for gravity). Finally, sika deer are very tame, easy to handle and to breed.

2.2 Research aims and hypotheses

This dissertation therefore aimed to use Sika deer antlers as a less invasive model to analyse the bone remodelling processes occurring around dental implants in different periods until complete osseointegration of the implants was achieved and the antlers were shed. A self-developed autonomous loading device (Rahimi et al., 2009) was used and enabled an *in vivo* analysis under an IL situation without sacrificing the animals or altering the normal behaviour of the deer. Micro-computed tomography (µCT) and histological analyses were used to reveal changes in bone structure and density during healing and to understand the general ossification process and the specific reaction of bone around implants. Finite element (FE) analyses were used to compare the displacements and stresses of implant, stresses and strains of antler tissue around the implant. This study would lay a theoretical basis for developing an alternative animal model for studying bone remodelling around dental implants.

2.3 Materials and Methods

2.3.1 Animal selection

Six healthy 4-year-old male captive bred and tamed Sika deer (Cervus nippon) were utilised in this study. The median weight of the animals was 64 kg (all 50-70 kg). All animals were handled according to the policies and principles established by the German Animal Welfare Act and approved by the North Rhine-Westphalia State Agency for Nature, Environment and Consumer Protection as the competent authority (Permission No.: LANUV NRW, 84-02.04.2014.A462). The investigations have been carried out based on the revised Declaration of Helsinki from the World Medical Association (1983) and its appropriate legal requirements.

2.3.2 Animal preparation and the surgical procedure

The animals were intramuscularly anaesthetised with 1.2 - 1.5 ml of Hellabrunn Mixture (100 mg of Ketamine and 125 mg of Xylazine per ml, Hafner et al., 1989) via distance immobilisation using a carbon dioxide injection gun (DAN-INJECT JM Standard injection rifle, DAN-INJECT Smith GmbH, Walsrode, Germany, Caulkett et al., 2007). After placing the deer on a surgical table in right lateral recumbency, anaesthesia was monitored by a visual inspection of breathing, auscultation of the heart and lungs, continuous monitoring of the rectal temperature and pulse oximetry (LifeVet P, Eickemeyer Medizintechnik für Tierärzte KG, Tuttlingen, Germany). A continuous oxygen supply was ensured by the use of a nasal tube and a flow rate between 1 and 5 l/min, depending on the breathing and oxygen parameters. A continuous intravenous drip infusion was applied via the lateral saphenous vein. The non-steroidal, anti-inflammatory agent meloxicam (Meloxidyl 20 mg/ml ad us vet., Ceva Tiergesundheit, Düsseldorf, Germany) was injected intramuscularly. In addition, local analgesia was applied by injecting 3 - 5 ml of lidocaine beneath branches of the zygomatic nerve at the antler's base (Lidocain 2%, B. Braun Melsungen, Melsungen, Germany, Walsh and Wilson, 2002; Wilson et al., 2000).

Before surgically raising the velvet from an area close to branches of the antler, disinfection was repeated with 70% alcohol and a 1% iodine tincture (Applichen GmbH, Darmstadt, Germany) and then a longitudinal incision of 5 cm was performed without releasing cuts to raise the velvet of both side up to 1 cm distance to the longitudinal incision. The implant sites were prepared by sequential drilling with a Ø 2.2 mm and a Ø 2.8 mm cylindrical twist drill and 800 U/min under sterile saline irrigation according to the manufacturers protocol.

In five animals (deer no. 1 - 5), two Straumann-Standard Plus Roxolid® soft tissue level implants (Institut Straumann AG, Basel, Switzerland) with a length of 10 mm and a diameter of 3.3 mm were inserted without thread-cutting in the left antler of each deer. The distance between two implants was 2.5 cm. Roxolid® is a titanium-zirconium alloy composed of about 15% zirconium and about 85% titanium and has been specifically designed for use in dental implantology (Chiapasco et al., 2012). The first implant received a ball abutment for transvelvet healing and the second received a closure screw. The tissues collected from the antlers of the sixth animal (deer no. 6, control animal that did not receive an implant) using a trepan drill were used as a control. The velvet was finally sutured using Serafit 4/0 (SERAG-WIESSNER GmbH & Co. KG, Naila, Germany) and subsequently covered by a Hansaplast spray bandage (Beiersdorf AG, Hamburg, Germany). The first implant was immediately vertically loaded via the custom-made loading device fixed with bone screws (Rahimi et al., 2009), whereas the second implant remained unloaded as control implant. The self-developed load control unit was attached to the right antler and the implants were loaded with vertical forces of 10 N at a frequency of 0.2 Hz. Consecutive loading cycles of 1 hour and unloaded periods of 5 hours were set. The details are given in Figure 1 of study 1, 2 and 3.

2.3.3 Follow-up and sample removal from the deer

Post-operatively, the animals and wounds were inspected daily for the absence of wound healing complications, alterations in general health, abnormal behaviours and reduced food intake. The correct placement of the loading devices was monitored daily. Animals were assigned randomly to different time points for implant removal, ranging from two to six weeks after surgery (deer no. 1: Two weeks post-operation; deer no. 2: Three weeks post-operation; deer no. 3: Four weeks post-operation; deer no. 4: Five weeks post-operation; and deer no. 5: Six weeks post-operation).

For this procedure, the animals were anaesthetised as described above and vertically loaded implants and the surrounding tissues were collected by using a trepan drill. The wound cavities were rinsed thoroughly and filled with a collagen sponge for local haemostasis (KOLLAGEN resorb, RESORBA Medical GmbH, Nuremberg, Germany). Finally, the velvet was sutured and the Hansaplast spray bandage was applied. Loading devices and the load control unit were removed. The unloaded implants were kept in place and collected after antler shedding in February of the next year to investigate the osseointegration of the implants in a fully-grown antler and the structure of antler tissue in comparison to human bone. Collected samples were immediately fixed in buffered formalin (4%) and subjected to µCT scanning and subsequent analyses.

2.3.4 Antler density analysis

The specimens were scanned in a µCT scanner (SkyScan 1174, SkyScan Bruker-microCT, Kontich, Belgium) at 50 kV, 800 µA, and a rotation step of 0.25°. A 1-mm-thick aluminium filter was used for beam-hardening reduction. The exposure time was set to 2 s. The scan times were approximately ten hours per sample. After scanning each sample, two calibration phantom rods (SkyScan, Kontich, Belgium) with bone mineral density (BMD) values of 0.25 and 0.75 g/cm^3 calcium hydroxyapatite was scanned on the same day using the same parameters. With the scans and reconstructions of the samples and the calibration phantoms complete, the BMD calibration program was performed by using Bruker-MicroCT CT-Analyser (SkyScan, Kontich, Belgium). First of all, the attenuation coefficient (AC) value of the two phantoms was measured and entered in the preferences histogram calibration table. BMD-AC formula was updated and the calibration was completed. Secondly, 3 mm peri-implant antler tissue was selected and the BMD was automatically calculated and recorded as mean ± standard deviation (SD).

2.3.5 Histological analysis

Antler samples with integrated implants were fixed in formaldehyde, dehydrated and infiltrated with ultraviolet light-activated polymethylmethacrylate (PMMA, Technovit 72100®, Heraeus Kulzer, Hanau, Germany) for one week. This procedure was followed by a 3 day immersion in a 1:1 combination of PMMA and 2-hydroxyethyl methacrylate (GMA, Heraeus Kulzer). After subsequent immersion in 100% embedding medium, the samples were photopolymerised under high-power UV light sources in three steps. Later, parallel 100 to 200 µm thick sections were cut from the specimens using a microsaw machine (EXAKT Advanced Technologies, Norderstedt, Germany) and sections up to 20 µm thickness were polished down using a micro grinding system (EXAKT). Sections obtained from the grinding system were stained using toluidine blue without removing the plastic medium and evaluated under a Zeiss-Axio-Imager® light microscope (Zeiss, Jena, Germany) at original magnifications ranging between 5 and 50x. These steps were performed in the Oral Biology Laboratory, University of Bonn.

2.3.6 Numerical analysis

The implant specimen that was taken after 2-week loading was not suitable for bone mineral density analysis, since the thickness of antler tissue around implant was less than 3 mm. For the unloaded implant samples, only three specimens were collected after the antler shedding. Therefore, the µCT data from the four loaded (3, 4, 5, and 6 weeks post-operatively) and three unloaded specimens were imported into Mimics research 19.0 and 3-Matic research 9.0 (Materialise NV, Leuven, Belgium) for 3D reconstruction. Thereafter, the models were converted into 3D FE models using 4-noded tetrahedral elements. The final models consisted of 235,297 up to 258,158 elements for the specimens retrieved 3, 4, 5 and 6 weeks after loading and 532,709 up to 1,116,651 elements for the unloaded models. The FE analysis was performed using the software package MSC.Marc/Mentat 2010 (MSC. Software, Santa Ana, CA, USA). All materials were assumed to be homogenous, isotropic and linearly elastic. Young's modulus of the antler tissue was calculated from the density using the following formula (Beaupré et al., 1990):

$$E=\begin{cases}2014\rho^{2.5} & \text{if } \rho\leq 1.25\ g/cm^3\\ 1763\rho^{3.2} & \text{if } \rho>1.25 g/cm^3\end{cases}.$$

The material properties of the implant were calculated for Roxolid® material (Young's modulus: 98 GPa; Poisson ratio: 0.3; Chiapasco et al., 2012). A frictional contact with a frictional coefficient of 0.3 was defined between the implant and the antler tissue to simulate the immediate loading condition (Tassani et al., 2011). Bonding contact was defined between antler tissue and implant for unloaded models to simulate osseointegrated condition. All models were constrained in all directions at the cutting surfaces and the bottom of the antler tissue. A linear vertical force of 10 N was applied on the implant. The magnitude of force was in agreement with that applied on loaded implants by the self-developed loading device. Static structure analysis was performed. The details are given in Figure 2 of study 2.

In the regions of maximum displacements, stresses and strains, ten nodes were randomly selected and the values were recorded respectively. The mean values of ten nodes were recorded as mean ± standard deviation (SD) and compared.

2.3.7 Statistical Evaluation

Data were analysed using IBM SPSS Statistics for Windows, version 20.0 software (IBM Corp., Armonk, NY, USA). One way ANOVA with the SNK (Student-Newman-Keuls) comparison test was used to explore the differences of displacements, stresses and strains among different loaded and unloaded specimens. SNK comparison was used because this study was an exploratory research. The displacements of implant, stresses of implant, stresses of antler tissue and strains of antler tissue in loaded and unloaded specimens in the same antler were compared using paired t-test. A significance level of 0.05 was chosen.

2.4 Results

2.4.1 Animal health and behaviour after implantation and loading

Signs of infections in the antler, behavioural changes and signs of impairment in the deer were not observed during the trial. The antlers of all animals were shed regularly during the subsequent spring and replaced by new and completely intact antlers within two to three months. Thus, the present trial did not disturb the normal behaviour of the deer or antler regeneration.

2.4.2 Number of specimens included in the analysis

For the specimens that were loaded for two weeks post-operatively, the thickness of antler tissue around implant was less than 3 mm, and not suitable for histological analysis and the study of bone mineral density as well. For this reason, four time points were selected for getting the samples out after IL namely, 3, 4, 5, and 6 weeks.

Only three unloaded implant samples were collected after the antler shedding due to the fact that it was difficult to find all the shedded antlers in a spacious activity place for Sika deer. Therefore, three unloaded specimens were included in the analysis.

2.4.3 Bone mineral density of antler tissue

The bone mineral density of antler tissue around the implant increased significantly during the healing period under IL conditions. BMD values observed at 3, 4, 5, and 6 post-operative weeks were 0.31 ± 0.01 g/cm^3, 0.92 ± 0.23 g/cm^3, 1.54 ± 0.40 g/cm^3, and 2.00 ± 0.53 g/cm^3, respectively. The BMD values observed at 6 post-operative weeks were similar to those for healthy adult human cortical bone (Tassani et al., 2011).

After shedding the antler, the BMD of antler tissue in specimens with unloaded implants were in a similar range (1.09 ± 0.24 g/cm^3, 1.26 ± 0.17 g/cm^3, 1.30 ± 0.11 g/cm^3). For deer no. 2, the BMD of antler tissue around the unloaded implant (1.26 ± 0.17 g/cm^3)

was higher than that around the 3-week loaded implant (0.31 ± 0.01 g/cm^3). Interestingly, in deer no. 5 the BMD of antler tissue around the 6-week loaded implant (2.00 ± 0.53 g/cm^3) was much higher than that around the unloaded implant (1.30 ± 0.11 g/cm^3). The details are given in study 1 and 2.

2.4.4 Histological results

For loaded specimens, osseointegration appeared to be insufficient in the specimens obtained at 3, 4 and 5 post-operative weeks. Peri-implant spaces with diameters up to 100 µm were observed along the implant bodies, ranging between half of the length and the entire length of the implant body. These spaces were filled with extravasations, blood cells, plaque and detritus. The peri-implant bone mostly consisted of a spongy or cancellous bone with good vascularisation. In the cervical and crestal regions of the implants, soft peri-implant tissue was present and probably originated from the pedicle skin or the periosteum of the antler. This soft tissue consisted of loose connective tissue covered by a multi-layered epithelium, focal round cell infiltration and granulation tissue. Osteogenesis was detected in the crestal region of the cancellous bone, particularly in specimens retrieved three and four weeks after surgery (deer nos. 2 and 3). However, similar to the unloaded implant specimens, the loaded implant specimen retrieved after six post-operative weeks exhibited very good osseointegration and a compact peri-implant bone with good vascularisation. Interestingly, the orientation of bone lamellation in the coronal areas was mainly longitudinal and parallel to the implant body axis, coinciding with the loading direction.

Specimens carrying unloaded implants collected after antler shedding displayed signs of excellent osseointegration. The peri-implant bone was mostly compact and peri-apically more cancellous with few fat marrow spaces. Growth was also visible in the crestal direction along the machined crestal implant surfaces. The crestal bony plateaus were smooth, contained only a thin layer of soft tissue remnants and showed no signs of bone resorption. A close bone contact forming a tight bone-implant interface was observed along the implant surface. At higher magnifications, e.g., 40x or 50x, single osteocytes were in very close proximity (maximal 5 µm) to the implant interface. Short and narrow peri-implant spaces of 10 to 20 µm were focally observed. Substantial vascularisation was observed in perforating channels and osteons near (maximal 10 µm) and distal to the implant surface. Two defects were evaluated after explantation of the implants to investigate the healing outcome. In both defects, small apically located tears and a small amount of detritus and small bony fragments were observed. A soft tissue layer with dense connective tissue covered the defect bone surfaces. The details are given in study 1.

2.4.5 Numerical results

Displacements of implants were concentrated at the neck of implants. The differences of maximum displacements of implants were significant among the three unloaded models and between the four loaded models. The highest and lowest values in the unloaded samples were observed with deer no. 1 (0.9 µm) and deer no. 2 (0.5 µm). For deer no. 2, the maximum displacements of the implant in the loaded model (3-week) were significantly higher than that in the unloaded model (P<.05). Conversely, in deer no. 5 significant higher values were obtained in the unloaded model compared with the loaded model (P<.05).

Stresses in antler tissue increased from 2.4 MPa (three weeks after surgery) to 6.5 MPa (five weeks after surgery) after IL and decreased to 1.7 MPa after 6 weeks of loading. The values in the unloaded models displayed a similar range (1.0 - 1.3 MPa). The distribution of the stresses in antler tissues for all models was similarly concentrated in the antler tissue around the neck of the implant. Both for deer no. 2 and no. 5, the maximum stresses in antler tissue in loaded models were significantly higher than that in the unloaded models (P<.05). In the 3-week loaded model (deer no. 2), the distribution of stresses in the antler tissue was concentrated in the antler tissue around the tip of the implant. For other models, the distribution of stresses in the antler tissue was similarly concentrated in the antler tissue around the neck of the implant.

Strain in the antler tissues decreased during the healing time for the loaded models, the 3-week (9,878 µstrain) and 6-week loaded models (49 µstrain), and illustrated the highest and the lowest maximum strain values among the antler tissues. The 3-week loaded model (deer no. 2) showed the widest distribution among all the models. For the models from deer no. 2, the maximum strain in the antler tissue in the loaded model was significantly higher than in the unloaded model ($P<.05$). In contrast, the opposite results were obtained in the models from deer no. 5. The details are given in study 2 and 3.

2.5 Discussion

Hard antlers are well suited mechanically since they are subject to high-impact loading and large bending moments (Chen et al., 2009; Currey et al., 2009; Kierdorf et al., 2013; Launey et al., 2010). The mechanical properties of hard antlers are highly anisotropic with the longitudinal elastic modulus, and higher bending, tensile and compressive strengths were observed in this direction than in the transverse direction (Rahimi et al., 2009). Antlers dry out completely following the shedding of velvet (Currey et al., 2009) and transform into dead structures with the absence of further growth or bone remodelling until antler replacement (Gomez et al., 2013).

Cortical porosity may vary along the main shaft (Gomez et al., 2013). The porosity is low in the lower and the middle thirds of the shaft due to the more rapid completion of cortex formation prior to velvet shedding (Gomez et al., 2013). The more distal parts of the antler may be more porous, as velvet shedding interrupts the ongoing mineralisation process in the primary osteons. Thus, cortical porosity in the antler may not be the result of remodelling activity but may be the result of incomplete bone formation (Gomez et al., 2013; Landete-Castillejos et al., 2012).

Antlers are predominantly composed of primary osteons (Skedros et al., 1995; Szuwart et al., 2002). In contrast, human bone is a secondary bone formed by the resorption of previously existing bone tissue and its replacement by new bone (Launey et al., 2010). This process results in the formation of secondary osteons (Landete-Castilleijos et al., 2007). All secondary osteons include a prominent hyper-mineralised region surrounding the primary osteons (Landete-Castilleijos et al., 2007; Skedros et al., 1995). In contrast, in human bone, a thin mineralised region, the cementum line, surrounds the secondary osteons (Skedros et al., 2005). Both types of osteons have strong implications for fractures and are prominent sites for microcracking (Burr et al., 1988; Launey et al., 2010; Yeni et al., 2000). However, the yield strength of antler compact bone in the transverse direction is as low as 71 MPa (Chen et al., 2009), whereas the corresponding yield strength of human cortical bone is approximately 110 to 120 MPa.

The results showed that the present trial did not disturb the normal behaviour of the deer or antler regeneration. Therefore, antlers can be safely used as a novel method for implantation research with a high value in terms of the refinement of the animal trial for research purposes. Implants are easily inserted into the deer antler using a clinical procedure with traditional implantation instruments. Loading was successful and well controlled when added onto the abutments by the self-developed loading devices. No implants were lost during the trial. Thus, the use of deer antlers combined with the novel loading device is a successful model for immediately loaded implant investigations.

Experimental specimens must be observed at different time intervals to understand the behaviour of the implants and the surrounding tissues after immediate loading. However, animals must be sacrificed to perform a histological analysis of the bone bed. Moreover, in traditional animal models, the load application on implants is difficult to control because the installation of the loading device in the mouth or on the top of other bone sites is affected by many factors such as food intake and physiological activity. In this study, a special self-developed loading device was placed externally on the antler and offered a good accessibility and an application of a specific, controlled load without the above-mentioned limiting factors. However, myiasis has to be prevented by a thorough velvet suture and application of a spray bandage at this external location, which would not have been a high risk inside the oral cavity. Using the loading device, the magnitude, direction and period of loading were controlled, thus avoiding other interfering factors and allowing the healing process to be monitored easily at different time intervals under immediate loading conditions.

After shedding the antler, the BMD of the antler tissue from the unloaded specimens exhibited a similar value of 1.30 ± 0.11 g/cm^3. These values were consistent with the results of the study by Chen *et al*. (2009), who discovered that the total bone density of the antler was 1.35 ± 0.01 g/cm^3. The antler density of the loaded specimens observed in this study was higher than in the unloaded specimens in single animals. Thus, the density of the antler tissue around the implant continuously increases over the loading period. However, the density might be reduced after the complete osseointegration of the implant, as shown in previous studies (Mainetti et al., 2015; Ramachandran et al., 2016), mainly influenced by the continuous remodelling process.

The histological results revealed excellent osseointegration, with a mostly compact peri-implant antler bone exhibiting growth in the crestal direction along the implant surfaces. This finding is comparable to studies using other animal models (Feng et al., 2016; Gottlow et al., 2012; Trisi et al., 2015). Based on these findings, the deer antler is a novel and valid animal model that simulates the clinical implant healing process.

The numerical results showed that the maximum values of displacements in implant and stresses and strains in antler tissue were significantly different among loaded models as well as among the unloaded models. This might be attributed to the various densities and geometries of the antler tissue in different animals. In the unloaded models with higher BMD and Young's modulus, strains in the antler tissue were lower. This is due to the reason that the deformation of the bone tissue by strain is inversely correlated to its stiffness. The higher the strain value, the lower the stiffness of the bone.

2.6 Conclusion

Implants inserted into Sika deer antler do not disturb the normal behaviour of the deer or antler regeneration. Density of the antler tissue around the implant goes up to higher values as the loading time increased, and remained in a similar range in the unloaded implants. The histological results revealed good osseointegration in unloaded and some loaded specimens, which is comparable to studies using other animal models.

Therefore, Sika deer antler might be a promising novel and valid animal model that simulates the clinical implant healing process.

2.7 References

Albrektsson T, Brånemark PI, Hansson HA, Lindström J. Osseointegrated titanium implants. Requirements for ensuring a long-lasting, direct bone-to-implant anchorage in man. Acta Orthop Scand 1981; 52: 155-170

Abboud M, Koeck B, Stark H, Wahl G, Paillon, R. Immediate loading of single-tooth implants in the posterior region. Int J Oral Maxillofac Implants 2005; 20: 61-68

Al-Sawai AA, Labib H. Success of immediate loading implants compared to conventionally-loaded implants: a literature review. J Investig Clin Dent 2016; 7: 217-224

Barndt P, Zhang H, Liu F. Immediate loading: from biology to biomechanics. Report of the Committee on Research in fixed Prosthodontics of the American Academy of fixed Prosthodontics. J Prosthet Dent 2015; 113: 96-107

Beaupré GS, Orr TE, Carterm DR. An approach for time-dependent bone modeling and remodeling-theoretical development. J. Orthop. Res. 1990; 8: 651-661

Brånemark PI. Osseointegration and its experimental background. J Prosthet Dent 1983; 50: 399-410

Burr DB, Schaffle MB, Frederickson RG. Composition of the cement line and its possible mechanical role as a local interface inhuman compact-bone. J Biomech 1988; 21: 939

Caulkett N, Haigh JC. Deer (Cervids). In: West G, Heard D, Caulkett N, editors. Zoo animal and wildlife immobilization and anaesthesia. Ames. Iowa: Blackwell Publishing, 2007: 607-612

Chen PY, Stokes AG, McKittrick J. Comparison of the structure and mechanical properties of bovine femur bone and antler of the North American elk (Cervus elaphus canadensis). Acta Biomater 2009; 5: 693-706

Chiapasco M, Casentini P, Zaniboni M, Corsi E, Anello T. Titanium-zirconium alloy narrow-diameter implants (Straumann Roxolid®) for the rehabilitation of horizontally deficient edentulous ridges: prospective study on 18 consecutive patients. Clin Oral Implants Res 2012; 23:1136-1141

Currey JD, Landete-Castillejos T, Estevez J, Ceacero F, Olguin A, Garcia A, Gallego L. The mechanical properties of red deer antler bone when used in fighting. J Exp Biol 2009; 212: 3985-3993

Feng SW, Ho KN, Chan YH, Chang KJ, Lai WY, Huang HM. Damping Factor as a Diagnostic Parameter for Assessment of Osseointegration during the Dental Implant Healing Process: an Experimental Study in Rabbits. Ann Biomed Eng 2016; 44: 3668-3678.

Gaspar-López E. Biometrics, testosterone, cortisol and antler growth cycle in Iberian red deer stags (Cervus elaphus hispanicus). Reprod Domest Anim 2010; 45: 243-249

Gomez JA, García AJ, Landete-Castillejos T, Gallego L. Effect of advancing births on testosterone until 2.5 years of age and puberty in Iberian red deer (Cervus elaphus hispanicus). Anim Reprod Sci 2006; 96: 79-88

Gomez S, Garcia AJ, Luna S, Kierdorf U, Kierdorf H, Gallego L, Landete-Castillejos T. Labeling studies on cortical bone formation in the antlers of red deer (Cervus elaphus). Bone 2013; 52: 506-515

Gottlow J, Dard M, Kjellson F, Obrecht M, Sennerby L. Evaluation of a new titanium-zirconium dental implant: a biomechanical and histological comparative study in the mini pig. Clin. Implant Dent Relat Res 2012; 14: 538-545

Götz W, Gedrange T, Bourauel C, Hasan I. Clinical, biomechanical and biological aspects of immediately loaded dental implants: a critical review of the literature. Biomed Tech (Berl) 2010; 55: 311-315

Hafner S, Wiesner H, von Hegel G, Halm S, Erhardt W. The antagonism of ketamine/xylazine anesthesia ("Hellabrunn mixture") in wild zoo ruminants. Berl Munch Tierartl 1989; 102: 181-184

Han J, Hou J, Zhou G, Wang C, Fan Y. A histological and biomechanical study of bone stress and bone remodeling around immediately loaded implants. Sci China Life Sci 2014; 6:618-626

Huang Y, van Dessel J, Martens W, Lambrichts I, Zhong WJ, Ma GW, Lin D, Liang X, Jacobs R. 2015. Sensory innervation around immediately vs. delayed loaded implants: a pilot study. Int J Oral Sci 7: 49-55

Kierdorf U, Stoffels E, Stoffels D, Kierdorf H, Szuwart T, Clemen G. Histological studies of bone formation during pedicle restoration and early antler regeneration in roe deer and fallow deer. Anat Rec A Discov Mol Cell Evol Biol 2003; 273: 741-751

Kunnekel AT, Dudani MT, Nair CK, Naidu EM, Sivagami G. Comparison of delayed implant placement vs immediate implant placement using resonance frequency analysis: a pilot study on rabbits. J Oral Implantol 2011; 5: 543-548

Landete-Castillejos T, Currey JD, Ceacero F, García AJ, Gallego L, Gomez S. Does nutrition affect bone porosity and mineral tissue distribution in deer antlers? The relationship between histology, mechanical properties and mineral composition. Bone 2012; 50: 245-254

Launey ME, Chen PY, McKittrick J, Ritchie RO. Mechanistic aspects of the fracture toughness of elk antler bone. Acta Biomater 2010; 6: 1505-1514

Li C, Suttie JM, Clark DE. Histological examination of antler regeneration in red deer (Cervus elaphus). Anat Rec A Discov Mol Cell Evol Biol 2005; 282: 163-174

Li C, Zhao H, Liu Z, McMahon C. Deer antler-a novel model for studying organ regeneration in mammals. Int J Biochem Cell Biol 2014; 56: 111-122

Mainetti T, Lang NP, Bengazi F, Sbricoli L, Soto Cantero L, Botticelli D. Immediate loading of implants installed in a healed alveolar bony ridge or immediately after tooth extraction: an experimental study in dogs. Clin Oral Implants Res 2015; 4: 435-441

Matin K, Senpuku H, Hanada N, Ozawa H, Ejiri S. Bone regeneration by recombinant human bone morphogenetic protein-2 around immediate implants: a pilot study in rats. Int J Oral Maxillofac Implants 2003; 2: 211-217

Meng S, Zhang X, Xu M, Heng BC, Dai X, Mo X, Wei JQ, Wei Y, Deng XL. Effects of deer age on the physicochemical properties of deproteinized antler cancellous bone: an approach to optimize osteoconductivity of bone graft. Biomed Mater 2015; 4: 035006

Rahimi A, Klein R, Keilig L, Abboud M, Wahl G, Bourauel C. Development and design of a novel loading device for the investigation of bone adaptation around immediately loaded dental implants using the reindeer antler as implant bed. J Biomech 2009; 42: 2415-2418

Ramachandran A, Singh K, Rao J, Mishra N, Jurel SK, Agrawal KK. Changes in alveolar bone density around immediate functionally and nonfunctionally loaded implants. J Prosthet Dent 2016; 115: 712-717

Trisi P, Berardini M, Falco A, Podaliri Vulpiani M. Effect of Implant Thread Geometry on Secondary Stability, Bone Density, and Bone-to-Implant Contact: a Biomechanical and Histological Analysis. Implant Dent 2015; 24: 384-391

Sato N, Kuwana T, Yamamoto M, Suenaga H, Anada T, Koyama S, Suzuki O, Sasaki K. Bone response to immediate loading through titanium implants with different surface roughness in rats. Odontology 2014; 7: 249-258

Skedros JG, Durand P, Bloebaum RD. Hypermineralized peripheral lamellae in primary osteons of deer antler: potential functional analogs of cement lines in mammalian secondary bone. J Bone Miner Res 1995; 10: S441

Simion M, Benigni M, Al-Hezaimi K, Kim DM. Early bone formation adjacent to oxidized and machined implant surfaces: a histologic study. Int J Periodontics Restorative Dent 2015 1: 9-17

Szuwart T, Kierdorf H, Kierdorf U, Clemen G. Histochemical and ultrastructural studies of cartilage resorption and acid phosphatase activity during antler growth in fallow deer (Dama dama). Anat Rec 2002; 268: 66-72

Tassani S, Ohman C, Baruffaldi F, Baleani M, Viceconti M. Volume to density relation in adult human bone tissue. J Biomech 2011; 44: 103-108

Vandamme K, Naert I, Geris L, Sloten JV, Puers R, Duyck J. Histodynamics of bone tissue formation around immediately loaded cylindrical implants in the rabbit. Clin Oral Implants Res 2007; 4:471-480

Walsh VP, Wilson PR. Chemical analgesia for velvet antler removal in deer. N. Z. Vet. J. 2002; 50: 237-243

Wilson PR, Stafford KJ, Thomas DJ, Mellor DJ. Evaluation of techniques for lidocaine hydrochloride analgesia of the velvet antlers of adult stags. N Z Vet J 2000; 48: 182-187

Yeni YN, Norman TL. Calculation of porosity and osteonal cement line effects on the effective fracture toughness of cortical bone in longitudinal crack growth. J Biomed Mater Res 2000; 51: 504-509

3.Publications

3.1 Study 1

Sika deer antler as a novel model to investigate dental implant healing:
A pilot experimental study

Yun He, Dominik Fischer, Istabrak Hasan, Werner Götz, Ludger Keilig, Luisa Ziegler, Markus Abboud, Christoph Bourauel, Gerhard Wahl

PLOS ONE 2018; 13(7): e0200957
doi: org/10.1371/journal.pone.0200957
Impact Factor ^{2017}: 2.766

RESEARCH ARTICLE

Sika deer antler as a novel model to investigate dental implant healing: A pilot experimental study

Yun He[1,2☯], Dominik Fischer[3,4☯], Istabrak Hasan[1,5]*, Werner Götz[6], Ludger Keilig[1,5], Luisa Ziegler[4], Markus Abboud[7], Christoph Bourauel[1], Gerhard Wahl[8]

1 Endowed Chair of Oral Technology, University of Bonn, Bonn, Germany, **2** Department of Oral Surgery, Hospital of Stomatology, Southwest Medical University, Luzhou, China, **3** Raptor Centre and Wildlife Park Hellenthal, Hellenthal, Germany, **4** Clinic for Birds, Reptiles, Amphibians and Fish, Veterinary Faculty, Justus Liebig University Giessen, Giessen, Germany, **5** Department of Prosthetic Dentistry, Preclinical Education and Materials Science, University of Bonn, Bonn, Germany, **6** Department of Orthodontics, Oral Biology Laboratory, University of Bonn, Bonn, Germany, **7** Department of Prosthodontics and Digital Technology, School of Dental Medicine, Stony Brook University, Stony Brook, New York, United States of America, **8** Department of Oral Surgery, University of Bonn, Bonn, Germany

☯ These authors contributed equally to this work.
* ihasan@uni-bonn.de

Check for updates

OPEN ACCESS

Citation: He Y, Fischer D, Hasan I, Götz W, Keilig L, Ziegler L, et al. (2018) Sika deer antler as a novel model to investigate dental implant healing: A pilot experimental study. PLoS ONE 13(7): e0200957. https://doi.org/10.1371/journal.pone.0200957

Editor: Jo-Ann L. Stanton, University of Otago, NEW ZEALAND

Received: February 28, 2018

Accepted: July 4, 2018

Published: July 31, 2018

Copyright: © 2018 He et al. This is an open access article distributed under the terms of the Creative Commons Attribution License, which permits unrestricted use, distribution, and reproduction in any medium, provided the original author and source are credited.

Data Availability Statement: All relevant data are within the paper and its Supporting Information files.

Funding: Following funding were involved in this study: Friadent GmbH (Mannheim, Germany) by sponsoring the implants for the initial investigations to improve the loading device. Straumann GmbH (Freiburg, Germany) by sponsoring the implants for the investigations in deer antlers. National Natural Science Foundation of China (11702231) by financial supporting for Mrs. Yun He. The funders did not have any

Abstract

Dental implants are important tools for restoring the loss of teeth. The rapid growth and periodic regeneration of antlers make Sika deer a good and less invasive alternative model for studying bone remodelling in mammals. We developed a special loading device for antlers and analysed the bone reaction around unloaded implants and under immediate loading conditions until osseointegration occurred. In micro-computed tomography images, the density of antler tissue around the implants increased as the loading time increased. This finding was histologically confirmed by the good osseointegration observed in unloaded and loaded specimens. Antler tissue displays a similar healing process to human bone. The use of an antler model is a promising alternative for implant studies that does not require animal sacrifice.

Introduction

Dental implants are important tools for restoring the loss of single teeth and fixing tooth implant-supported fixed partial dentures after accidents, disease or age-related loss of teeth [1]. Therefore, dental implants improve the quality of a patient's life by improving aesthetics and phonetics and by decreasing bone resorption processes in the alveolar ridge. In particular, immediately loaded dental implants offer fast dental restoration and pain relief [1,2]. Research regarding complex bone remodelling processes occurring around dental implants is crucial to improve the function and acceptance of dental implants. Therefore, *in vivo* models are required, and animal trials have previously been conducted in pigs and dogs that were

additional role in the study design, data collection and analysis, decision to publish, or preparation of the manuscript. The specific roles of these authors are articulated in the 'author contributions' section.

Competing interests: The authors declare the following interests: Materiel support in the form of implants for the investigations in deer antlers was provided by the commercial company Straumann GmbH (Freiburg, Germany). Material support in the form of implants for the initial investigations to improve the loading device was provided by the commercial company Friadent GmbH (Mannheim, Germany). There are no patents, products in development, or marketed products to declare. This does not alter the authors' adherence to all PLOS ONE policies on sharing data and materials.

ultimately sacrificed [3,4]. This limitation restricted an intensive investigation of bone tissue due to ethical reasons.

Deer antlers represent well-exposed and rapidly growing bones that change and regenerate periodically. Thus, antlers may be used as a good model for studying bone remodelling in mammals [5–10]. Antlers start to grow from bony pedicles located on the head of male Sika deer in winter or spring and are enveloped in vascularised velvet, the periosteum, during growth [11]. The growth rate may reach up to 1.2 cm per day during the 70 days of the fastest growth period [11]. In summer, growth ceases, and the antlers are completely mineralised; in addition, the velvet is shed, thereby exposing the bare bone of the so-called hard antlers from July to August [11,12]. The development of an abscission layer across the base induces casting of the antlers to complete the cycle and to enable subsequent regrowth [13–16].

In our study, we used Sika deer antlers as a less invasive model to analyse the bone remodelling processes occurring around dental implants in different periods until complete osseointegration of the implants was achieved, and the antlers were shed. The use of a self-developed autonomous loading device [17] enabled an *in vivo* analysis under an immediate loading situation without sacrificing the animals or altering the normal behaviour of the deer. Micro-computed tomography (μCT) and histological analyses were used to reveal changes in bone structure and density during healing and to understand the general ossification process and the specific reaction of bone around implants. Finite element analyses were used to observe the biomechanical properties of the implant and the surrounding antler tissue.

Materials and methods

Animal selection

Six healthy 4-year-old male captive bred and tamed Sika deer (Cervus nippon) were utilised in this study. The median weight of the animals was 64 kg (all 50–70 kg). All animals were handled according to the policies and principles established by the German Animal Welfare Act and approved by the North Rhine-Westphalia State Agency for Nature, Environment and Consumer Protection as the competent authority (Permission No.: LANUV NRW, 84–02.04.2014.A462).

Animal preparation and the surgical procedure

The animals were intramuscularly anaesthetised with 1.2–1.5 ml of Hellabrunn Mixture (100 mg of Ketamine and 125 mg of Xylazine per ml) [18] via distance immobilisation using a carbon dioxide injection gun (DAN-INJECT JM Standard injection rifle, DAN-INJECT Smith GmbH, Walsrode, Germany) [19]. After placing the deer on a surgical table in right lateral recumbency, anaesthesia was monitored by a visual inspection of breathing, auscultation of the heart and lungs, continuous monitoring of the rectal temperature and pulse oximetry (Life-Vet P, Eickemeyer Medizintechnik für Tierärzte KG, Tuttlingen, Germany). A continuous oxygen supply was ensured by the use of a nasal tube and a flow rate between 1 and 5 l/min, depending on the breathing and oxygen parameters. A continuous intravenous drip infusion was applied via the lateral saphenous vein. The non-steroidal, anti-inflammatory agent meloxicam (Meloxidyl 20 mg/ml ad us vet., Ceva Tiergesundheit, Düsseldorf, Germany) was injected intramuscularly. In addition, local analgesia was applied by injecting 3–5 ml of lidocaine beneath branches of the zygomatic nerve at the antler's base (Lidocaine 2%, B. Braun Melsungen, Melsungen, Germany, [20, 21].

Before surgically raising the velvet from two 1.5 × 1.5-cm^2-sized areas close to branches of the antler, disinfection was repeated with 70% alcohol and a 1% iodine tincture (Applichen GmbH, Darmstadt, Germany), and a longitudinal incision of 5 cm was then performed without releasing cuts to raise the velvet of both sides up to a 1-cm distance to the longitudinal incision. The implant sites were prepared by sequential drilling with a Ø 2.2-mm and a Ø 2.8-mm cylindrical twist drill and 800 U/min under sterile saline irrigation according to the manufacturer's protocol. In five animals (deer no. 1–5), two Straumann-Standard Plus Roxolid® soft tissue level implants (Institut Straumann AG, Basel, Switzerland) with a length of 10 mm and a diameter of 3.3 mm were inserted without thread-cutting in the left antler of each deer. The distance between the two implants was 2.5 cm. Roxolid® is a titanium-zirconium alloy composed of approximately 15% zirconium and approximately 85% titanium and has been specifically designed for use in dental implantology [22]. The first implant received a ball abutment for transvelvet healing, and the second received a closure screw. The tissues collected from the antlers of the sixth animal (deer no. 6, control animal that did not receive an implant) using a trepan drill were used as a control. The velvet was finally sutured using Serafit 4/0 (SERAG-WIESSNER GmbH & Co. KG, Naila, Germany) and was subsequently covered with a Hansaplast spray bandage (Beiersdorf AG, Hamburg, Germany). The first implant was immediately vertically loaded via the custom-made loading device fixed with bone screws [17], whereas the second implant remained unloaded (Fig 1). The self-developed load control unit was attached to the right antler. No loading device was placed in the control animal.

Follow-up and sample removal from the deer

Post-operatively, the animals and wounds were inspected daily for the absence of wound healing complications, alterations in general health, abnormal behaviours and reduced food intake. The correct placement of the loading devices was monitored daily. Animals were assigned randomly to different time points for implant removal, ranging from 3 to 6 weeks after surgery (deer no. 2: 3 weeks post-operation; deer no. 3: 4 weeks post-operation; deer no. 4: 5 weeks post-operation; and deer no. 5: 6 weeks post-operation). For this procedure, the animals were anaesthetised as described above, and vertically loaded implants and the surrounding tissues were collected using the trepan drill. The wound cavities were rinsed thoroughly and filled with a collagen sponge for local haemostasis (KOLLAGEN resorb, RESORBA Medical GmbH, Nuremberg, Germany). Finally, the velvet was sutured, and the Hansaplast spray bandage was applied. Loading devices and the load control unit were removed. The unloaded implants were kept in place and collected after antler shedding in February of the next year to investigate the osseointegration of the implants in a fully grown antler and the structure of antler tissue in comparison to human bone. Collected samples were immediately fixed in buffered formalin (4%) and subjected to μCT scanning and subsequent analyses.

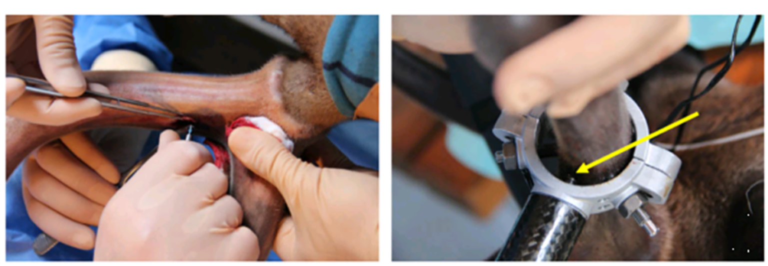

Fig 1. Dental implant inserted into the Sika deer antler and loaded. Insertion of a dental implant into the Sika deer antler (left). Each animal (deer no. 1–5) received two implants at a position near the branching point of the antler. One of the implants was loaded by an autonomous loading device controlled by a micro-computer. The implant was loaded by a motor driven thrust die (yellow arrow).

https://doi.org/10.1371/journal.pone.0200957.g001

Antler density analysis

Specimens collected from antlers 3, 4, 5 and 6 weeks after implant insertion were used in this study to analyse changes in antler density at different healing periods. The specimens were scanned in a micro-computed tomography (μCT) scanner (SkyScan 1174, SkyScan Bruker-microCT, Kontich, Belgium) at 50 kV, 800 μA, and a rotation step of 0.25˚. A 1-mm-thick aluminium filter was used for beam-hardening reduction. The exposure time was set to 2 s. The scan times were approximately 10 hours per sample. After scanning each sample, two calibration phantom rods (SkyScan, Kontich, Belgium) with bone mineral density (BMD) values of 0.25 and 0.75 g/cm^3 calcium hydroxyapatite were scanned on the same day using the same parameters. With the scans and reconstructions of the samples and the calibration phantoms complete, the BMD calibration program was performed using a Bruker-MicroCT CT-Analyser (SkyScan, Kontich, Belgium). First, the attenuation coefficient (AC) value of the two phantoms was measured and entered in the preferences histogram calibration table. The BMD-AC formula was updated, and the calibration was completed. Second, 3 mm of peri-implant antler tissue was selected, and the BMD was automatically calculated and recorded as the mean ± standard deviation (SD).

Histological analysis

Antler samples with integrated implants were fixed in formaldehyde, dehydrated and infiltrated with ultraviolet light-activated polymethylmethacrylate (PMMA, Technovit 72100®, Heraeus Kulzer, Hanau, Germany) for one week. This procedure was followed by a 3-day immersion in a 1:1 combination of PMMA and 2-hydroxyethyl methacrylate (GMA, Heraeus Kulzer). After subsequent immersion in 100% embedding medium, the samples were photopolymerised under high-power UV light sources in three steps. Later, parallel 100- to 200-μm-thick sections were cut from the specimens using a microsaw machine (EXAKT Advanced Technologies, Norderstedt, Germany), and sections up to 20 μm in thickness were polished down using a micro grinding system (EXAKT). Sections obtained from the grinding system were stained using toluidine blue without removing the plastic medium and were evaluated under a Zeiss-Axio-Imager® light microscope (Zeiss, Jena, Germany) at original magnifications ranging between 5 and 50x.

Numerical analysis

The μCT data from the four loaded and three unloaded specimens were imported into Mimics research 19.0 and 3-Matic research 9.0 (Materialise NV, Leuven, Belgium) for 3D reconstruction. Thereafter, the models were converted into 3D finite element (FE) models using 4-noded tetrahedral elements. The final models consisted of 235,297–258,158 elements for the specimens retrieved 3, 4, 5 and 6 weeks after loading and 532,709–1,116,651 elements for the unloaded models (Fig 2). The FE analysis was performed using the software package MSC. Marc/Mentat 2010 (MSC. Software, Santa Ana, CA, USA). All materials were assumed to be homogenous, isotropic and linearly elastic. Young's modulus of the antler tissue was calculated from the density using the following formula [23]:

$$E = \begin{cases} 2014\rho^{2.5} & \text{if } \rho \leq 1.25\ \text{g/cm}^3 \\ 1763\rho^{3.2} & \text{if } \rho > 1.25\ \text{g/cm}^3 \end{cases}$$

The material properties of the implant were calculated for Roxolid® material (Young's modulus: 98 GPa; Poisson's ratio: 0.3; 22). A frictional contact with a frictional coefficient of

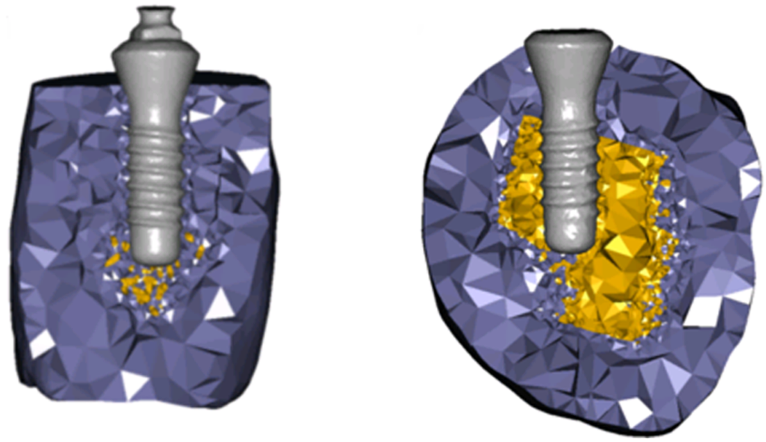

Fig 2. Example of finite element models of the specimens with and without loading. FE models created 6 weeks after loading (left); and an unloaded specimen from the same antler (right).

https://doi.org/10.1371/journal.pone.0200957.g002

0.3 was defined between the implant and the antler tissue to simulate the immediate loading condition [24]. All models were constrained in all directions at the cutting surfaces and the bottom of the antler tissue. A linear vertical force of 10 N was applied on the implant. Stresses and strains were evaluated and compared for all of the models using the software package MSC.Marc/Mentat 2010.

Results

Animal health and behaviour after implantation and loading

Signs of infections in the antler, behavioural changes and signs of impairment in the deer were not observed during the trial. The antlers of all animals were shed regularly during the subsequent spring and were replaced with new and completely intact antlers within 2–3 months. Thus, the present trial did not disturb the normal behaviour of the deer or antler regeneration.

Number of specimens included in the analysis

For the specimens that were loaded for 2 weeks post-operatively, the thickness of the antler tissue around the implant was less than 3 mm and was not suitable for histological analysis or BMD study. For this reason, four time points were selected for removing the samples after immediate loading, namely, 3, 4, 5 and 6 weeks.

Only three unloaded implant samples were collected after antler shedding due to the difficulty finding all the shed antlers in the Sika deer's activity space. Therefore, three unloaded specimens were included in the analysis.

Bone mineral density of antler tissue

The BMD of antler tissue around the implant increased significantly during the healing period under immediate loading conditions. The BMD values observed at 3, 4, 5 and 6 post-operative weeks were 0.31 ± 0.01 g/cm^3, 0.92 ± 0.23 g/cm^3, 1.54 ± 0.40 g/cm^3 and 2.00 ± 0.53 g/cm^3, respectively. The BMD values observed at 6 post-operative weeks were similar to those for healthy adult human cortical bone [24]. For unloaded specimens, the BMD values for antler tissue were lower than those for loaded implants. For example, in the deer segment obtained 6 weeks after implant insertion, the BMD values of antler tissue were 1.30 ± 0.11 g/cm^3 around the unloaded implant and 2.00 ± 0.53 g/cm^3 around the loaded implant.

Histological results

Unloaded specimens

Specimens carrying unloaded implants collected after antler shedding displayed signs of excellent osseointegration (Figs 3 and 4). The peri-implant bone was mostly compact and peri-apically more cancellous with few fat marrow spaces. Growth was also visible in the crestal direction along the machined crestal implant surfaces (Fig 3). The crestal bony plateaus were smooth, contained only a thin layer of soft tissue remnants and showed no signs of bone resorption. A close bone contact forming a tight bone-implant interface was observed along the implant surface. At higher magnifications, e.g., 40 or 50x, single osteocytes were in very close proximity (maximal 5 μm) to the implant interface (Fig 4a–4c). Short and narrow peri-implant spaces of 10–20 μm were focally observed (Fig 4d). Substantial vascularisation was observed in perforating channels and osteons near (maximal 10 μm) and distal to the implant surface. Two defects were evaluated after explantation of the implants to investigate the healing outcome. In both defects, small apically located tears, a small amount of detritus and small bony fragments were observed. A soft tissue layer with dense connective tissue covered the defect bone surfaces.

Loaded specimens

Osseointegration appeared to be insufficient in the specimens obtained at 3, 4 and 5 post-operative weeks. Peri-implant spaces with diameters up to 100 μm were observed along the implant bodies, ranging between half of the length and the entire length of the implant body. These spaces were filled with extravasations, blood cells, plaque and detritus. The peri-implant bone mostly consisted of a spongy or cancellous bone with good vascularisation. In the cervical and crestal regions of the implants, soft peri-implant tissue was present and likely originated from the pedicle skin or the periosteum of the antler. This soft tissue consisted of loose connective tissue covered by a multi-layered epithelium, focal round cell infiltration and granulation

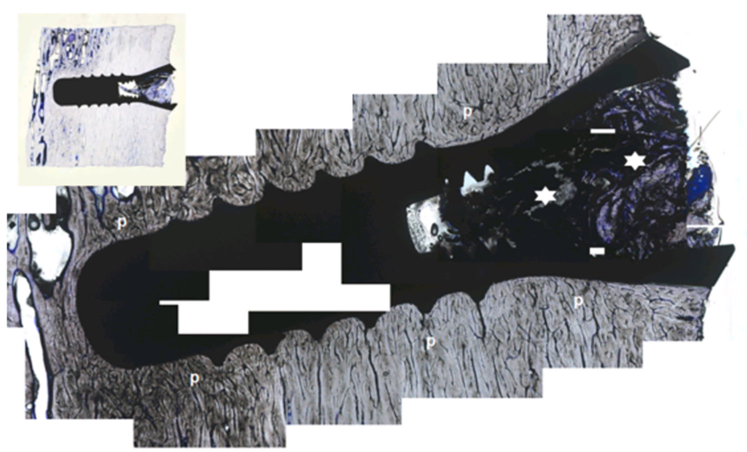

Fig 3. Unloaded implant in a Sika deer antler after 6 weeks from insertion. p = Peri-implant bone, asterisks = artefacts and detritus in the inside taper; toluidine blue staining, reconstruction and 5x magnification; Inset: overview of the inserted implant; 1:1.

https://doi.org/10.1371/journal.pone.0200957.g003

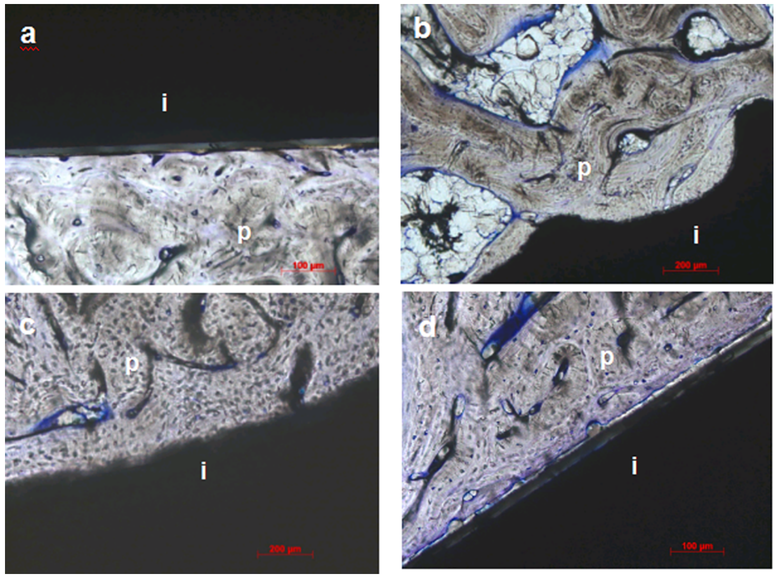

Fig 4. Detailed images of the interfaces from the unloaded implants in the Sika deer antler. a) High-magnification image of cortical peri-implant bone (midshaft), b) high-magnification image of periapical cancellous bone (images in both a and b were captured 3 weeks after insertion), c) high-magnification images of cortical peri-implant bone (crestal) and d) the peri-implant gap (crestal, images in both c and d were captured 6 weeks after insertion); toluidine blue staining, 10x magnification (b), 20x magnification (a, c and d); p = peri-implant bone, i = implant.

https://doi.org/10.1371/journal.pone.0200957.g004

tissue. Osteogenesis was detected in the crestal region of the cancellous bone, particularly in specimens retrieved 3 and 4 weeks after surgery (deer nos. 2 and 3). However, similar to the unloaded implant specimens, the loaded implant specimen retrieved at 6 post-operative weeks exhibited very good osseointegration and a compact peri-implant bone with good vascularisation (Figs 5 and 6). Interestingly, the orientation of bone lamellation in the coronal areas was mainly longitudinal and parallel to the implant body axis (Fig 6).

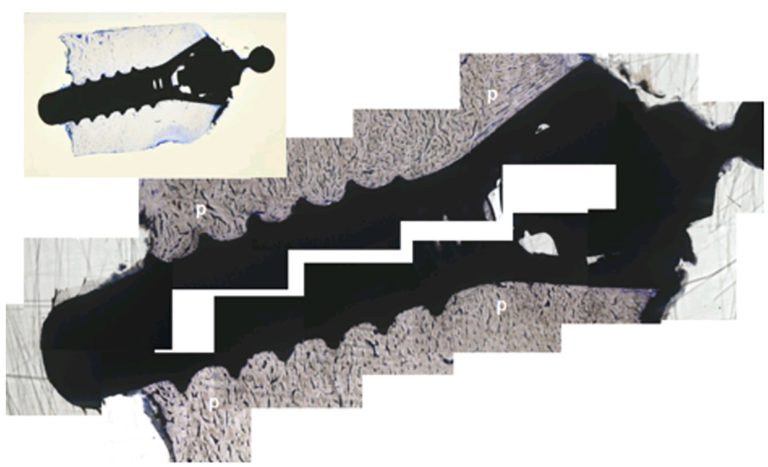

Fig 5. The loaded implant in the Sika deer antler 6 weeks after insertion. p = peri-implant bone; toluidine blue staining, reconstruction, and 5x magnification; Inset: overview of the inserted implant; 1:1.

https://doi.org/10.1371/journal.pone.0200957.g005

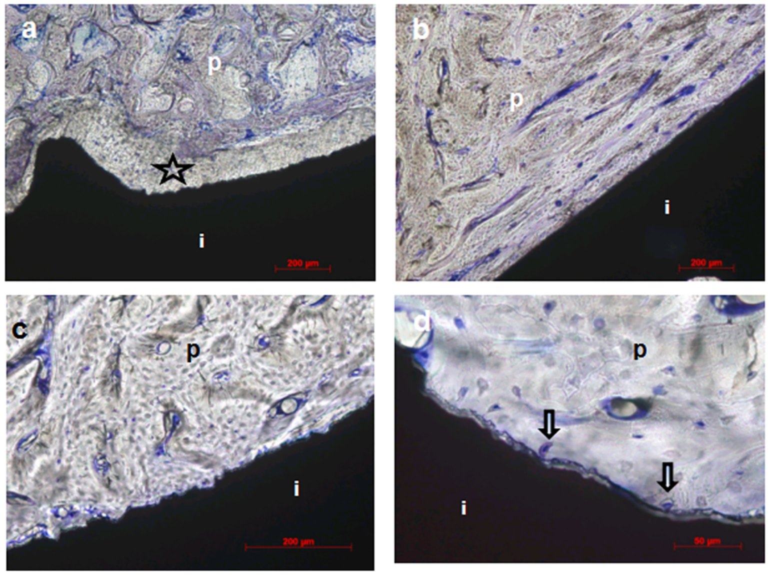

Fig 6. Detailed images of the interfaces from loaded implants in a Sika deer antler. a) Peri-implant gap along the implant body at 3 weeks after insertion, star: gap; b) high-magnification image of the compact bone along the midshaft implant surface at 6 weeks after insertion; c) high-magnification image of the compact bone as in b); please note the abundance of blue stained vessels in the peri-implant bone in b) and c). d) Osteocytes of the peri-implant bone are in close contact with the implant surface (open arrows) at 6 weeks after insertion; toluidine blue staining, 10x magnification (a and b), 20x magnification (c), 50x magnification (d); p = peri-implant bone, i = implant.

https://doi.org/10.1371/journal.pone.0200957.g006

Numerical results

To evaluate the stress and strain, a 3-mm peri-implant antler tissue was selected. Stresses in antler tissue increased from 2.4 MPa (3 weeks after surgery) to 6.5 MPa (5 weeks after surgery) after immediate loading and decreased to 1.7 MPa after 6 weeks of loading. The values in the unloaded models displayed a similar range (1.0–1.3 MPa). The distribution of the stresses in antler tissues for all models was similarly concentrated in the antler tissue around the neck of the implant.

Strain in antler tissues decreased during the healing time for the loaded models, the 3-week (9,878 μstrain) and 6-week loaded models (49 μstrain), and illustrated the highest and lowest maximum strain values among the antler tissues. For the models from deer no. 2, the maximum strain in antler tissue in the loaded model was higher than that in the unloaded model. In contrast, the opposite results were obtained in the models from deer no. 5 (Fig 7).

Discussion

Hard antlers are well suited mechanically since they are subject to high-impact loading and large bending moments [10,13,25,26]. The mechanical properties of hard antlers are highly anisotropic with the longitudinal elastic modulus, and higher bending, tensile and compressive strengths are observed in this direction than in the transverse direction [17]. Antlers dry out completely following the shedding of velvet [13] and transform into dead structures with the absence of further growth or bone remodelling until antler replacement [27].

Cortical porosity may vary along the main shaft [27]. The porosity is low in the lower and middle thirds of the shaft due to the more rapid completion of cortex formation prior to velvet shedding [27]. The more distal parts of the antler may be more porous, as velvet shedding interrupts the ongoing mineralisation process in the primary osteons. Thus, cortical porosity

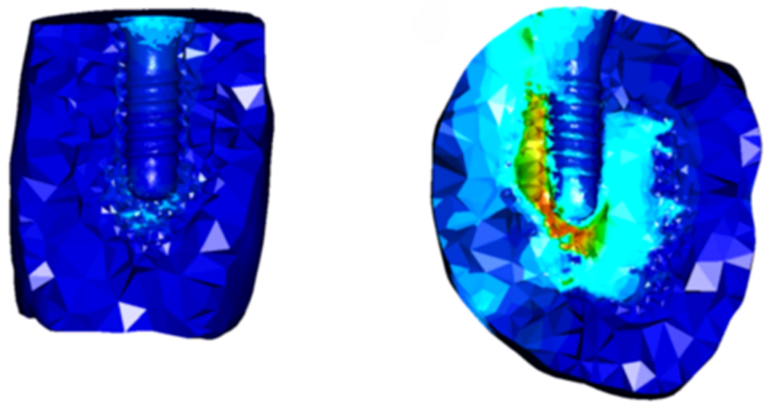

Fig 7. Example of strain in antler tissues in loading and unloaded models. Strains observed in the antler tissues 6 weeks after loading (left) and in the unloaded specimen from the same antler (right).

https://doi.org/10.1371/journal.pone.0200957.g007

in the antler may not be the result of remodelling activity but may be the result of incomplete bone formation [16,27].

Antlers are predominantly composed of primary osteons [15,28]. In contrast, human bone is a secondary bone formed by the resorption of previously existing bone tissue and its replacement by new bone [26]. This process results in the formation of secondary osteons [29]. All secondary osteons include a prominent hyper-mineralised region surrounding the primary osteons [28,29]. In contrast, in human bone, a thin mineralised region, the cementum line, surrounds the secondary osteons [30]. Both types of osteons have strong implications for fractures and are prominent sites for microcracking [26,31,32]. However, the yield strength of antler compact bone in the transverse direction is as low as 71 MPa [25], whereas the corresponding yield strength of human cortical bone is approximately 110–120 MPa.

The results showed that the present trial did not disturb the normal behaviour of the deer or antler regeneration. Therefore, antlers can be safely used as a novel method for implantation research with a high value in terms of the refinement of the animal trial for research purposes. Implants are easily inserted into the deer antler using a clinical procedure with traditional implantation instruments. Loading was successful and well controlled when added onto the abutments by self-developed loading devices. No implants were lost during the trial. Thus, the use of deer antlers combined with the novel loading device is a successful model for immediately loaded implant investigations.

Experimental specimens must be observed at different time intervals to understand the behaviour of the implants and surrounding tissues after immediate loading. However, animals must be sacrificed to perform a histological analysis of the bone bed. Moreover, in traditional animal models, the load application on implants is difficult to control because the installation of the loading device in the mouth or on top of other bone sites is affected by many factors such as food intake and physiological activity. In this study, a special self-developed loading device was placed externally at the antler and offered good accessibility and the application of a specific load without the abovementioned limiting factors. However, myiasis was prevented by a thorough velvet suture and application of a spray bandage at this external location, which would not have been a high risk inside the oral cavity. Using the loading device, the magnitude, direction and period of loading were controlled, thus avoiding other interfering factors and allowing the healing process to be monitored easily at different time intervals under immediate loading conditions.

After shedding the antler, the BMD of antler tissue from the unloaded specimens exhibited a similar value of 1.30 ± 0.11 g/cm^3. These values were consistent with the results of the study by Chen *et al.* [25], who discovered that the total bone density of the antler was 1.35 ± 0.01 g/cm^3. The antler density of the loaded specimens observed in this study was higher than that of the unloaded specimens in single animals. Thus, the density of the antler tissue around the implant continuously increases over the loading period. However, the density might be reduced after the complete osseointegration of the implant, as shown in previous studies [33,34].

The histological results revealed excellent osseointegration, with a mostly compact peri-implant antler bone exhibiting growth in the crestal direction along the implant surfaces. This finding is comparable to those of studies using other animal models [35–37]. Based on these findings, the deer antler is a novel and valid animal model that simulates the clinical implant healing process.

The deformation of the bone tissue by strain is inversely correlated to its stiffness. The higher the strain value, the lower the stiffness of the bone. The strain in the antler tissues of the loaded model was noticeably lower than that in the unloaded model. Thus, the osseointegration process of implants is faster under the loading condition than under the non-loading condition. These results are very important and present the deer antler as a novel, valid animal model to simulate the clinical implant healing process.

Supporting information

S1 File. The ARRIVE guidelines checklist.
(DOCX)

Acknowledgments

The authors thank the staff of Raptor Center and Wildlife Parc Hellenthal, especially Mr Joerg Niesters, Mr Karl Fischer, Mr Dirk Wynands and Dr Martin Boettcher, for the care of the animals. The authors also thank the staff of the Endowed Chair of Oral Technology, University of Bonn, Dr Susanne Reimann and Ms Anna Weber for preparing and scanning the specimens by µCT scanner, and Mr Tim Klunter for removing the specimens from the antlers.

Author Contributions

Conceptualization: Istabrak Hasan, Gerhard Wahl.

Data curation: Ludger Keilig.

Formal analysis: Yun He, Ludger Keilig.

Funding acquisition: Gerhard Wahl.

Investigation: Yun He.

Project administration: Dominik Fischer, Werner Götz, Markus Abboud, Christoph Bourauel, Gerhard Wahl.

Software: Ludger Keilig.

Supervision: Luisa Ziegler, Christoph Bourauel, Gerhard Wahl.

Writing – original draft: Yun He.

Writing – review & editing: Yun He, Dominik Fischer, Werner Götz, Christoph Bourauel, Gerhard Wahl.

References

1. Abboud M, Koeck B, Stark H, Wahl G, Paillon R. Immediate loading of single-tooth implants in the posterior region. Int. J. Oral Maxillofac. Implants. 2005; 20: 61–68. PMID: 15747675
2. Götz W, Gedrange T, Bourauel C, Hasan I. Clinical, biomechanical and biological aspects of immediately loaded dental implants: a critical review of the literature. Biomed. Tech. (Berl). 2010; 55: 311–315.
3. Rea M, Lang NP, Ricci S, Mintrone F, González G, Botticelli D. Healing of implants installed in over- or under-prepared sites: an experimental study in dogs. Clin. Oral Implants Res. 2015; 26: 442–426. https://doi.org/10.1111/clr.12390 PMID: 24684411
4. Alharbi HM, Babay N, Alzoman H, Basudan S, Anil S, Jansen JA. Bone morphology changes around two types of bone-level implants installed in fresh extraction sockets: a histomorphometric study in Beagle dogs. Clin. Oral Implants Res. 2015; 26, 1106–1112. https://doi.org/10.1111/clr.12388 PMID: 24690000
5. Goss RJ. Epimorphic regeneration in mammals. In: Hunt TK, Heppenstall RB, Pines E, Rovee RB, editors. Soft and Hard Tissue Repair. New York: Praeger; 1984. pp.554–573.
6. Bubenik GA. The antler as a model in biomedical research. In: Bubenik GA, Bubenik AB, editors. Horns, Pronghorns, and Antlers. New York: Springer; 1990. pp.474–487.
7. Price JS, Allen S, Faucheux C, Althnaian T, Mount JG. Deer antlers: a zoological curiosity or the key to understanding organ regeneration in mammals? J. Anat. 2005; 207: 603–618. https://doi.org/10.1111/j.1469-7580.2005.00478.x PMID: 16313394
8. Kierdorf U, Li C, Price JS. Improbable appendages: deer antler renewal as a unique case of mammalian regeneration. Semin. Cell Dev. Biol. 2009; 20: 535–542. https://doi.org/10.1016/j.semcdb.2008.11.011 PMID: 19084608
9. Kierdorf U, Kierdorf H. Deer antlers: a model of mammalian appendage regeneration: an extensive review. Gerontology. 2011; 57: 53–65. https://doi.org/10.1159/000300565 PMID: 20332600
10. Kierdorf U, Flohr S, Gomez S, Landete-Castillejos T, Kierdorf H. The structure of pedicle and hard antler bone in the European roe deer (Capreolus capreolus): a light microscope and backscattered electron imaging study. J. Anat. 2013; 223: 364–384. https://doi.org/10.1111/joa.12091 PMID: 23961846
11. Gaspar-López E. Biometrics, testosterone, cortisol and antler growth cycle in Iberian red deer stags (Cervus elaphus hispanicus). Reprod. Domest. Anim. 2010; 45: 243–249. https://doi.org/10.1111/j.1439-0531.2008.01271.x PMID: 18992114
12. Gomez JA, García AJ, Landete-Castillejos T, Gallego L. Effect of advancing births on testosterone until 2.5 years of age and puberty in Iberian red deer (Cervus elaphus hispanicus). Anim. Reprod. Sci. 2006; 96: 79–88. https://doi.org/10.1016/j.anireprosci.2005.11.008 PMID: 16406397
13. Currey JD, Landete-Castillejos T, Estevez J, Ceacero F, Olguin A, Garcia A, et al. The mechanical properties of red deer antler bone when used in fighting. J. Exp. Biol. 2009; 212: 3985–3993. https://doi.org/10.1242/jeb.032292 PMID: 19946076
14. Meng S, Zhang X, Xu M, Heng BC, Dai X, Mo X, et al. Effects of deer age on the physicochemical properties of deproteinized antler cancellous bone: an approach to optimize osteoconductivity of bone graft. Biomed Mater. 2015; 4: 035006.
15. Szuwart T, Kierdorf H, Kierdorf U, Clemen G. Histochemical and ultrastructural studies of cartilage resorption and acid phosphatase activity during antler growth in fallow deer (Dama dama). Anat. Rec. 2002; 268: 66–72. https://doi.org/10.1002/ar.10135 PMID: 12209566
16. Landete-Castillejos T, Currey JD, Ceacero F, García AJ, Gallego L, Gomez S. Does nutrition affect bone porosity and mineral tissue distribution in deer antlers? The relationship between histology, mechanical properties and mineral composition. Bone. 2012; 50: 245–254. https://doi.org/10.1016/j.bone.2011.10.026 PMID: 22071000
17. Rahimi A, Klein R, Keilig L, Abboud M, Wahl G, Bourauel C. Development and design of a novel loading device for the investigation of bone adaptation around immediately loaded dental implants using the reindeer antler as implant bed. J. Biomech. 2009; 42: 2415–2418. https://doi.org/10.1016/j.jbiomech.2009.06.032 PMID: 19733856
18. Hafner S, Wiesner H, von Hegel G, Halm S, Erhardt W. The antagonism of ketamine/xylazine anesthesia (" Hellabrunn mixture") in wild zoo ruminants. Berl. Munch. Tierartl. 1989; 102: 181–184.
19. Caulkett N, Haigh JC. Deer (Cervids). In: West G, Heard D, Caulkett N, editors. Zoo animal and wildlife immobilization and anaesthesia. Ames. Iowa: Blackwell Publishing; 2007. pp. 607–612.
20. Wilson PR, Stafford KJ, Thomas DJ, Mellor DJ. Evaluation of techniques for lidocaine hydrochloride analgesia of the velvet antlers of adult stags. N. Z. Vet. J. 2000; 48: 182–187. https://doi.org/10.1080/00480169.2000.36190 PMID: 16032150

21. Walsh VP, Wilson PR. Chemical analgesia for velvet antler removal in deer. N. Z. Vet. J. 2002; 50: 237–243. https://doi.org/10.1080/00480169.2002.36319 PMID: 16032279

22. Chiapasco M, Casentini P, Zaniboni M, Corsi E, Anello T. Titanium-zirconium alloy narrow-diameter implants (Straumann Roxolid(®)) for the rehabilitation of horizontally deficient edentulous ridges: prospective study on 18 consecutive patients. Clin Oral Implants Res. 2012; 23:1136–41. https://doi.org/10.1111/j.1600-0501.2011.02296.x PMID: 22092806

23. Beaupré GS, Orr TE, Carterm DR. An approach for time-dependent bone modeling and remodeling-theoretical development. J. Orthop. Res. 1990; 8: 651–61. https://doi.org/10.1002/jor.1100080506 PMID: 2388105

24. Tassani S, Ohman C, Baruffaldi F, Baleani M, Viceconti M. Volume to density relation in adult human bone tissue. J. Biomech. 2011; 44: 103–108. https://doi.org/10.1016/j.jbiomech.2010.08.032 PMID: 20850118

25. Chen PY, Stokes AG, McKittrick J. Comparison of the structure and mechanical properties of bovine femur bone and antler of the North American elk (Cervus elaphus canadensis). Acta. Biomater. 2009; 5: 693–706. https://doi.org/10.1016/j.actbio.2008.09.011 PMID: 18951859

26. Launey ME, Chen PY, McKittrick J, Ritchie RO. Mechanistic aspects of the fracture toughness of elk antler bone. Acta. Biomater. 2010; 6:1505–1514. https://doi.org/10.1016/j.actbio.2009.11.026 PMID: 19941980

27. Gomez S, Garcia AJ, Luna S, Kierdorf U, Kierdorf H, Gallego L, et al. Labeling studies on cortical bone formation in the antlers of red deer (Cervus elaphus). Bone. 2013; 52: 506–515. PMID: 23000508

28. Skedros JG, Durand P, Bloebaum RD. Hypermineralized peripheral lamellae in primary osteons of deer antler: potential functional analogs of cement lines in mammalian secondary bone. J. Bone Miner. Res. 1995; 10: S441.

29. Landete-Castilleijos T, Currey JD, Estevez JA, Gasparlópez E, Garcia A, Gallego L. Influence of physiological effort of growth and chemical composition onantler bone mechanical properties. Bone. 2007; 41: 794. PMID: 17822969

30. Skedros JG, Holmes JL, Vajda EG, Bloebaum RD. Cement lines of secondary osteons in human bone are not mineral-deficient: new data in a historical perspective. Anat. Rec. A. 2005; 286A: 781.

31. Burr DB, Schaffle MB, Frederickson RG. Composition of the cement line and its possible mechanical role as a local interface inhuman compact-bone. J. Biomech. 1988; 21: 939. PMID: 3253280

32. Yeni YN, Norman TL. Calculation of porosity and osteonal cement line effects on the effective fracture toughness of cortical bone in longitudinal crack growth. J. Biomed. Mater. Res. 2000; 51: 504. PMID: 10880095

33. Ramachandran A, Singh K, Rao J, Mishra N, Jurel SK, Agrawal KK. Changes in alveolar bone density around immediate functionally and nonfunctionally loaded implants. J. Prosthet. Dent. 2016; 115: 712–717. https://doi.org/10.1016/j.prosdent.2015.11.013 PMID: 26803180

34. Mainetti T, Lang NP, Bengazi F, Sbricoli L, Soto Cantero L, Botticelli D. Immediate loading of implants installed in a healed alveolar bony ridge or immediately after tooth extraction: an experimental study in dogs. Clin. Oral Implants Res. 2015; 4: 435–441.

35. Feng SW, Ho KN, Chan YH, Chang KJ, Lai WY, Huang HM. Damping Factor as a Diagnostic Parameter for Assessment of Osseointegration during the Dental Implant Healing Process: an Experimental Study in Rabbits. Ann. Biomed. Eng. 2016; 44: 3668–3678. https://doi.org/10.1007/s10439-016-1675-6 PMID: 27307008

36. Trisi P, Berardini M, Falco A, Podaliri Vulpiani M. Effect of Implant Thread Geometry on Secondary Stability, Bone Density, and Bone-to-Implant Contact: a Biomechanical and Histological Analysis. Implant Dent. 2015; 24: 384–391. https://doi.org/10.1097/ID.0000000000000269 PMID: 25939083

37. Gottlow J, Dard M, Kjellson F, Obrecht M, Sennerby L. Evaluation of a new titanium-zirconium dental implant: a biomechanical and histological comparative study in the mini pig. Clin. Implant Dent. Relat. Res. 2012; 14: 538–545. https://doi.org/10.1111/j.1708-8208.2010.00289.x PMID: 20586785

3.2 Study 2

Biomechanical Characteristics of Immediately Loaded and Osseointegration Dental Implants Inserted into Sika Deer Antler

Yun He, Istabrak Hasan, Ludger Keilig, Dominik Fischer, Luisa Ziegler, Markus Abboud, Gerhard Wahl, Christoph Bourauel

Medical Engineering and Physics 2018; 59(9): 8-14
doi: 10.1016/j.medengphy.2018.04.021
Impact Factor ^{2017}: 1.923

Medical Engineering and Physics 59 (2018) 8–14

Contents lists available at ScienceDirect

Medical Engineering and Physics

journal homepage: www.elsevier.com/locate/medengphy

Biomechanical characteristics of immediately loaded and osseointegration dental implants inserted into Sika deer antler

Yun He[a,b], Istabrak Hasan[b,c,*], Ludger Keilig[b,c], Dominik Fischer[d,e], Luisa Ziegler[e], Markus Abboud[g], Gerhard Wahl[f], Christoph Bourauel[b]

[a] Orofacial Reconstruction and Regeneration Laboratory, Department of Oral and Maxillofacial Surgery, the Hospital of Stomatology, Southwest Medical University, Luzhou, China
[b] Oral Technology, Dental School, University of Bonn, Welschnonnenstr. 17, 53111 Bonn, Germany
[c] Department of Prosthetic Dentistry, Preclinical Education and Materials Science, Dental School, University of Bonn, Bonn, Germany
[d] Raptor Center and Wildlife Parc Hellenthal, Hellenthal, Germany
[e] Clinic for Birds, Reptiles, Amphibians and Fish, Veterinary Faculty, Justus Liebig University Giessen, Giessen, Germany
[f] Department of Oral Surgery, Dental School, University of Bonn, Bonn, Germany
[g] Department of Prosthodontics and Digital Technology, School of Dental Medicine, Stony Brook University, 1104 Westchester Hall, Stony Brook, New York

ARTICLE INFO

Article history:
Received 30 September 2017
Revised 13 March 2018
Accepted 16 April 2018

Keywords:
Implant
Sika deer antler
Immediate loading
Osseointegration
Stress

ABSTRACT

This study aimed to compare biomechanical characteristics of immediately loaded (IL) and osseointegrated (OS) dental implants inserted into Sika deer antler and lay a foundation for developing an alternative animal model for dental implants studies. Two implants per antler were inserted. One implant was loaded immediately via a self-developed loading device; the other was submerged and unloaded as control. IL implants were harvested after different loading periods. The unloaded implants were collected after OS and the shedding of antler. Specimens were scanned by μCT scanner and finite element models were generated. A vertical force of 10 N was applied on the implant. The mean values of maximum displacements, stresses and strains were compared. The results showed that the density of antler tissue around the implants dramatically increased as the loading time increased. After shedding the antler, 3 pairs of antlers were collected and the density of antler tissue remained in a similar value in all specimens. The maximum values of displacement and stresses in implant and stresses and strains in antler tissue were significantly different among OS models. In one antler, all the biomechanical parameters of IL model were significantly higher than those of OS model of the same animal ($P < 0.05$) and wider distributions were obtained from IL model. It can be concluded that implants inserted into Sika deer antler might not disturb the growth and calcification process of antler and the use of Sika deer antler model is a promising alternative for implant studies that does not require animal sacrifice.
© 2018 IPEM. Published by Elsevier Ltd. All rights reserved.

1. Introduction

With the worldwide growing of aging population, there has been considerable increase in the demand for the replacement of lost teeth by means of implant-retained restorations over the last few decades. The clinical success of implant therapy is based on osseointegration, defined as the direct contact between living bone and the implant without the interposition of fibrous tissue [1–3]. Conventionally, loading on implant-retained restoration should be avoided before osseointegration. However, immediately loaded (IL) implants which allow for shorter rehabilitation times have shown similar implant stability and success rate compared with traditional delayed loading implants. Some studies showed that IL is beneficial to delayed loading, since loading is capable of stimulating the healing process [4–6]. IL implants appear to increase patient satisfaction and avoid the difficulty of wearing a conventional temporary restoration during the healing phase as well [7]. Thus, there is a trend in using an immediate loading protocol for implant-retained restoration currently.

While animal models closely represent the mechanical and physiological human clinical situation, they have been widely used in investigating dental implants in loaded or unloaded situations over potentially long time spans and in different tissue qualities (e.g., normal healthy or osteoporotic bone) and ages [8]. Each animal model has unique advantages and disadvantages; therefore for

* Corresponding author at: Oral Technology, Department of Prosthetic Dentistry, Preclinical Education and Materials Science, Dental School, University of Bonn, Welschnonnenstr. 17, 53111 Bonn, Germany.
E-mail address: ihasan@uni-bonn.de (I. Hasan).

https://doi.org/10.1016/j.medengphy.2018.04.021
1350-4533/© 2018 IPEM. Published by Elsevier Ltd. All rights reserved.

different purposes there are numerous models for testing the properties of implant and its surrounding tissue in vivo. Specifically, for studies investigating bone remodeling process around IL implants, the animal model should have similar bone characteristics to human bone and be appropriate for inserting implants and applying loadings [9]. However, the main disadvantages for the existing animal models are the uncontrolled loads that are exerted on the implants and the sacrificed fate of animals. For these reasons, exploring a novel animal model that is able to apply a controlled force on the inserted IL implant and does not interfere with the animals' behavior is admirable.

Deer are the only mammals that are capable of fully regenerating a complex organ, called antlers [10]. The ability to fully regenerate stands out as the most impressive feature of antlers. The repeated regeneration each year is even more remarkable, because mammalian appendages are generally considered as being incapable of regeneration. Deer antlers grow annually in defiance of what could be considered nature's rules [11]. The annual cycle of antler growth starts in spring. After the rapid elongation and the formation of lateral branches in summer, antler gradually becomes calcified in late summer or autumn. The process of calcification is initiated from the base of the antler and proceeds up through the antler and finishes when the distal ends of the tines form sharp tips [11]. After the calcification process has been completed, in conjunction with the loss of blood vessels and nerves, the velvet skin is shed. In winter, the bare bony antlers are firmly attached to the living pedicle and are not "cast" until the following spring. Antler casting triggers another round of antler regeneration [12]. This cycle provides a relative reasonable time span for investigating bone remodeling processes around implants inserted into the antler without sacrificing the animal. Besides, deer antlers are similar to human bones in regard to chemical composition and physiological structure [13,14]. Furthermore, as a muscle- and joint-free bony cranial appendage [15,16], antlers provide a fascinating model to investigate bone remodeling process around IL implant without the influence of external forces (except for gravity).

The primary aim of this study was to compare bone remodeling and biomechanical characteristics of immediately loaded and osseointegrated dental implants inserted into Sika deer antler. Secondly, the aim was to lay a theoretical foundation for developing an alternative animal model for studying bone remodelling around dental implants.

2. Materials and methods

2.1. Animal welfare statement

All animals were handled according to the policies and principles established by the German animal welfare act (TSchG, last amended on 3rd December 2015), approved by the North Rhine-Westphalia State Agency for Nature, Environment and Consumer Protection as competent authority (Permission No.: LANUV NRW, 84-02.04.2014.A462).

2.2. Surgery procedure

In July of 2015, six 4-year-old male Sika deer (bred at Wildlife Parc Hellenthal, Germany) were anesthetized using 1.2–1.5 ml Hellabrunn's mixture (100 mg Ketamine and 125 mg Xylazine per ml) according to standard procedures [17,18]. After disinfection and additional local anaesthesia with 3–5 ml lidocaine (Lidocain B. Braun 2%, B. Braun Melsungen, Melsungen, Germany), a longitudinal incision was performed and velvet flap elevated. Implant site was prepared at a position near a branching of the antler by sequential drilling under sterile saline irrigation according to the surgical protocol. Two implants per antler were inserted in a distance of 2.5 cm. The implants were Straumann Roxolid® soft tissue level implants (Institut Straumann AG, Basel, Switzerland) with a length of 10 mm and a diameter of 3.3 mm. After suturing the incision, the most proximal implant was vertically loaded immediately via a self-developed screw retained loading device [19], while the other one remained unloaded as a control. The motor of the control electronics were fixed on the other antler by colored bandages. Bandage with the different colors, blue, orange, yellow, red and black were used to distinguish the animals (Fig. 1). One deer was dead during the anesthetisation phase. After 2, 3, 4, 5 and 6 weeks, respectively, the loaded implants and surrounding tissue were randomly taken out with a trephine from one animal and the wounds were filled with bone wax (Ethicon®-bone wax, Johnson and Johnson, Hamburg, Germany), sutured and bandage protected. The samples were fixed in buffered formalin (4%). The unloaded implants remained in the antler for osseointegration. In winter, the antlers were collected after their shedding. Finally only three pairs of antlers, blue, orange and black, were able to be collected. The other two pairs of antlers could not be found. Thereafter, the unloaded implant with surrounding antler tissue and the antler tissue adjacent to the former specimen were sectioned for further investigation.

2.3. Numerical analysis

Specimens were prepared and scanned in a µCT scanner (SkyScan 1174, Bruker-micro CT, Kontich, Belgium) using 50 kV and 800 μA, rotation step of 0.25°. Data sets were reconstructed. After scanning the sample, calibration phantom with known density of calcium hydroxyapatite (SkyScan 1174, Bruker-microCT, Kontich, Belgium) was scanned on the same day by using the same parameters. Bone mineral density (BMD) of antler tissue (including cortical and trabecular bone) was calculated by using Bruker-Micro CT-Analyser (Bruker-micro CT, Kontich, Belgium).

µCT data of the specimens with implant were imported into Mimics research 18.0 (Materialise NV, Leuven, Belgium). Later on, three masks were created by defining different Hounsfield range, including the mask of implant, antler tissue (including cortical bone and trabecular bone) and bone marrow. After reconstruction, data were further processed in 3-Matic research 10.0 (Materialise NV, Leuven, Belgium) and converted into 3D finite element (FE) models using 4-noded tetrahedral elements. The final models of unloaded implant consisted of 532,709; 1,116,651; and 819,677 elements in specimens of blue, orange and black antler, respectively (Fig. 2). The 3D FE analysis was performed using the software package MSC.Marc/Mentat 2010 (MSC. Software, Santa Ana, CA, USA).

All materials were assumed to be isotropic and linear elastic. Young's modulus of the antler tissue was calculated by using the formula [20]:

$$E = \begin{cases} 2014\rho^{2.5} \ if \ \rho \le 1.25 \ g/cm^3 \\ 1763\rho^{3.2} \ if \ \rho > 1.25 \ g/cm^3 \end{cases}$$

Material properties of the implant (Roxolid® material) and bone marrow that were used in the analysis were taken from the literature (Table 2) [21,22].

Friction contact (frictional coefficient $\mu = 0.3$) was defined between antler tissue and implant for IL models. Osseointegrated condition was simulated between antler tissue and implant for unloaded (OS) models.

All models were constrained in all directions at the nodes on the lateral sides and bottom of the antler segment. Analog to the loading behavior of the implants in deer antler, a vertical force of 10 N, was applied onto the implant. In the regions of maximum

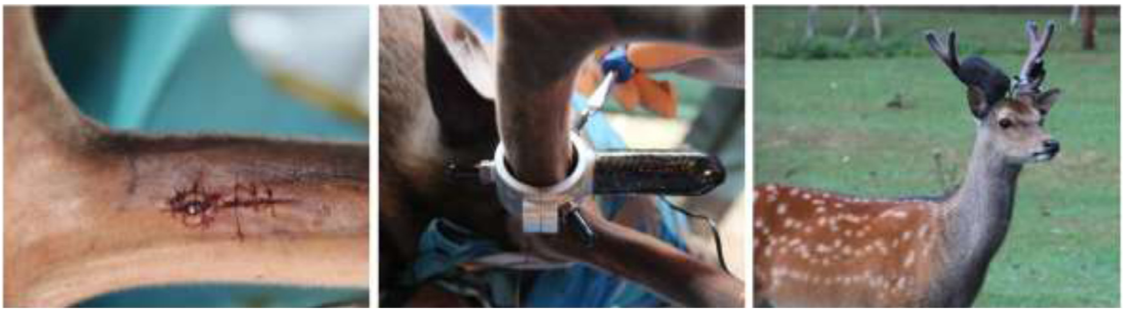

Fig. 1. Each animal received two implants at a position near a branching of the antler (left). One of the implants was loaded by an autonomous loading device, and the second one was submerged and remained unloaded (middle). An example of colored bandage (black) was used to fix the motor of the lading device (right).

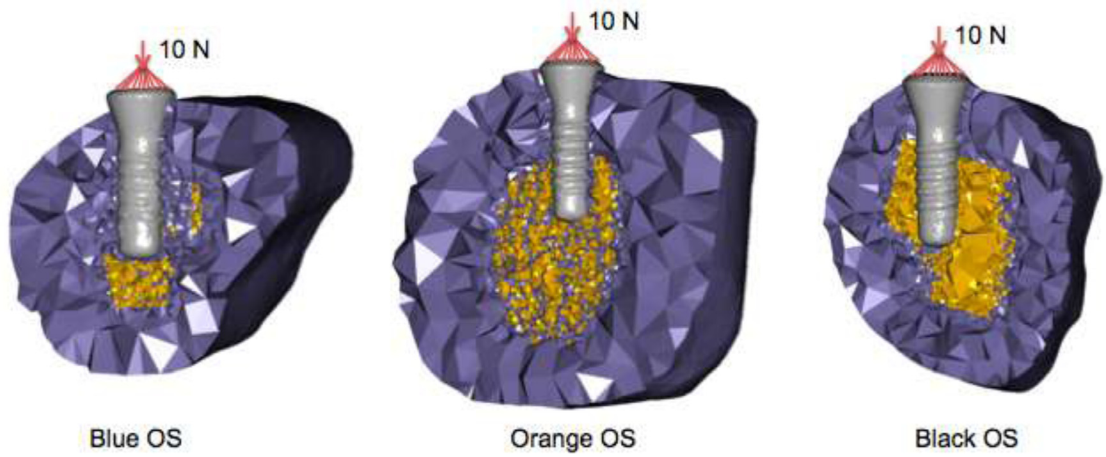

Fig. 2. Finite element models of blue, orange, and black Sika deer antler segments.
Grey: implant; blue: original antler tissue around the implant in the samples; yellow: bone marrow.

displacements, stresses and strains, ten nodes were randomly selected and the values were recorded respectively. The mean values of ten nodes were recorded as mean ± standard deviation (SD) and compared.

2.4. Statistical evaluation

Data were analysed using IBM SPSS Statistics for Windows, version 20.0 software (IBM Corp., Armonk, NY, USA). One way ANOVA with the SNK comparison test was used to explore the differences of displacements, stresses and strains among different osseointegration specimens. Independent Samples *t*-test was used to compare the differences of displacements, stresses and strains between the two IL specimens. The biomechanical values of OS and IL specimens in the same animal were compared using paired *t*-test. A significance level of 0.05 was chosen.

3. Results

3.1. BMD and Young's modulus of the antler tissue

Deer with blue, orange, yellow, red and black bandage, respectively, received 2, 3, 4, 5, 6 weeks immediately loading. As the loading time increased, BMD of antler tissue surrounding the implant dramatically increased. After shedding the antler, the BMD of antler tissue in specimens with osseointegrated implants (blue: 1.09 g/cm^3, orange: 1.26 g/cm^3, black: 1.30 g/cm^3) and without implants (blue: 1.28 g/cm^3, orange: 1.20 g/cm^3, black: 1.31 g/cm^3) were in a similar range. For orange antler, the BMD of antler tissue around OS implant was higher than that around IL implant. Interestingly, in black antler the BMD of antler tissue around IL implant (2.00 g/cm^3) was much higher than that around OS implant (1.30 g/cm^3). The BMD of specimens and corresponding material properties of the numerical models were shown in Tables 1 and 2.

Table 1
Bone mineral density (BMD, g/cm^3) of the antler tissue around implants at different healing periods.

Deer antler	Specimen		
	IL	OS with implant	OS without implant
Blue (2-week)	–	1.09 ± 0.24	1.28 ± 0.18
Orange (3-week)	0.31 ± 0.01	1.26 ± 0.17	1.20 ± 0.12
Yellow (4-week)	0.92 ± 0.23	–	–
Red (5-week)	1.54 ± 0.40	–	–
Black (6-week)	2.00 ± 0.53	1.30 ± 0.11	1.31 ± 0.13

IL: Immediately loaded implant specimen, OS with implant: Osseointegration implant specimen, OS without implant: The specimen of antler tissue without implant adjacent to the osseointegration implant specimen.

Table 2
Material properties of the numerical models.

Material	Young's modulus (MPa)	Poisson ratio
Blue Antler tissue (OS)	2487	0.30
Orange Antler tissue (3-week IL)	108	0.30
Orange Antler tissue (OS)	3665	0.30
Black Antler tissue (6-week IL)	16,200	0.30
Black Antler tissue (OS)	4092	0.30
Roxolid®	98,000	0.30
Bone marrow	2	0.16

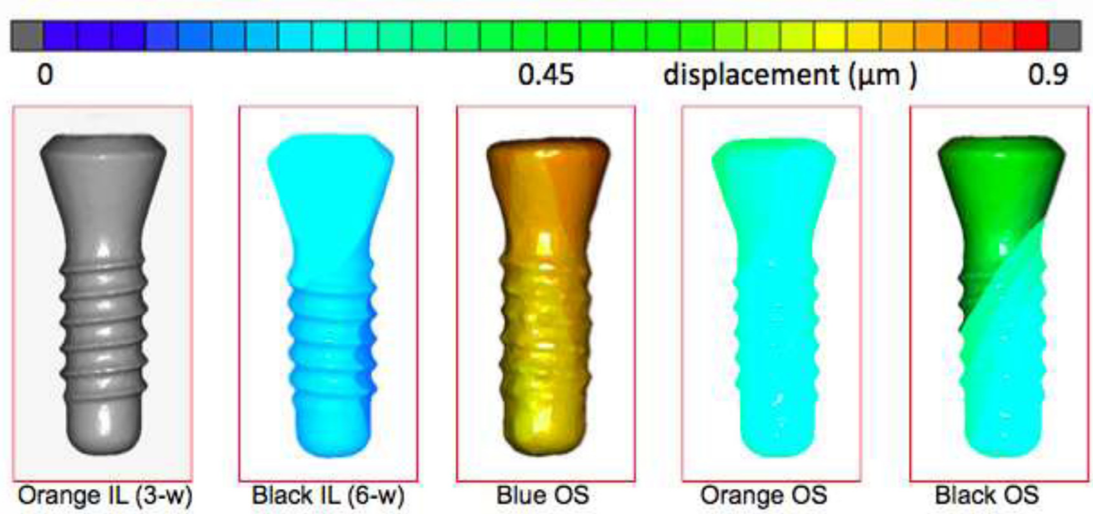

Fig. 3. Stress distributions in implant for IL-models and OS-models. Orange IL (3-w): model of orange antler with immediately loaded implant for 3 weeks; black IL (6-w): model of black antler with immediately loaded implant for 6 weeks; blue OS: model of blue antler with unloaded implant; orange OS: model of orange antler with unloaded implant; black OS: model of black antler with unloaded implant.

Table 3
Obtained maximum values of displacements (μm) in implants in immediate loading (IL) and osseointegrated (OS) models with different postoperative time.

	IL	OS	*t*	*P* value
Blue (2-week)	–	0.9 ± 0.1		
Orange (3-week)	6.2 ± 0.3	0.5 ± 0.1[a]	57.3	<0.001
Black (6-week)	0.4 ± 0.1	0.6 ± 0.1[a,b]	−2.9	0.018
F/*t*	59.6	55.2	–	–
P value	<0.001	<0.001		

[a] $P < 0.05$, when compared with blue.
[b] $P < 0.05$, when compared with orange.

Table 4
Obtained maximum values of stresses in implant (MPa) in immediate loading (IL) and osseointegrated (OS) models in different postoperative time.

	IL	OS	*t*	*P* value
Blue (2-week)	–	1.0 ± 0.1		
Orange (3-week)	2.8 ± 0.1	1.2 ± 0.1[a]	29.6	<0.001
Black (6-week)	2.5 ± 0.0	0.9 ± 0.1[b]	62.3	<0.001
F/*t*	11.7	10.0	–	–
P value	<0.001	0.001		

[a] $P < 0.05$, when compared with blue.
[b] $P < 0.05$, when compared with orange.

3.2. FE results

The differences of maximum displacement of implants were significant among the three OS models (Table 3). The highest and lowest values in OS samples were observed with blue antler (0.9 μm) and orange antler models (0.5 μm). The maximum displacement of the implant in orange antler IL model was significantly higher than that in orange antler OS model ($P < 0.05$). Conversely, in black antler models significant higher values were obtained in OS model compared with IL model ($P < 0.05$).

Stresses in the implant were significantly different among the OS models (Table 4), and the distribution was concentrated in the neck of implant. The highest values of stresses in the implant were observed in OS models (1.2 MPa) and wider distribution was founded in orange antler model (Fig. 3). There were no significant differences between blue and black antler OS models ($P > 0.05$). Both for orange and black antler models, the maximum stresses of the implant in IL models were significantly higher than that in OS models ($P < 0.05$). The distribution of IL models was wider than that of OS models.

Table 5
Obtained maximum values of stresses (MPa) in antler tissue in osseointegrated (OS) and immediate loading (IL) models with different postoperative time.

	IL	OS	*t*	*P* value
Blue (2-week)		1.0 ± 0.1		
Orange (3-week)	2.4 ± 0.8	1.1 ± 0.1[a]	4.9	0.001
Black (6-week)	6.5 ± 1.5	1.3 ± 0.2[a]	10.7	<0.001
F/*t*	−7.5	7.9	–	–
P value	<0.001	0.002		

[a] $P < 0.05$, when compared with blue.

The stress in antler tissue was increased from 2.4 MPa (3 weeks after IL) to 6.5 MPa (5 weeks after IL) in IL models. Stresses in antler tissue were considerably different among OS models, and the distribution was similarly concentrated in the antler tissue around the neck of implant (Table 5, Fig. 4). For OS models, the highest and lowest values of maximum stresses in antler tissue were observed in black antler (1.3 MPa) and blue antler models (1.0 MPa). Both for orange and black antler models, the maximum stresses in antler tissue in IL models were significantly higher than that in OS models ($P < 0.05$).

Maximum strain in antler tissues was decreased from 9879 μstrain to 363 μstrain during the healing time for the IL models. Among OS models, the highest values of strains in antler tissue were detected in blue antler OS model (1888 μstrain), followed by orange antler (686 μstrain) and black antler OS models (523 μstrain). The blue antler OS model also showed the widest distribution of strains in antler tissue. The differences among them were significant ($P < 0.05$). For orange antler models, the maximum strains in antler tissue in IL models were significantly higher than that in OS models ($P < 0.05$). In contrast, the opposite results were obtained in black antler models (Table 6, Fig. 6).

4. Discussion

Studies indicated that implant loading can be performed immediately or early after insertion without disturbing the biological osseointegration process and can be beneficial for peri-implant bone

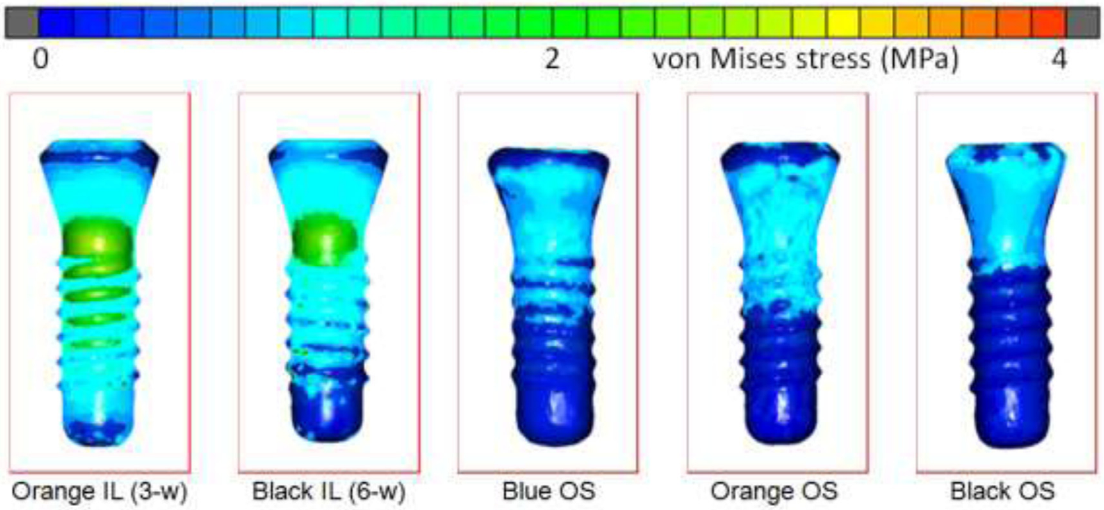

Fig. 4. Stress distributions in the antler tissue for IL-models and OS-models. Orange IL (3-w): model of orange antler with immediately loaded implant for 3 weeks; black IL (6-w): model of black antler with immediately loaded implant for 6 weeks; blue OS: model of blue antler with unloaded implant; orange OS: model of orange antler with unloaded implant; black OS: model of black antler with unloaded implant.

implant.

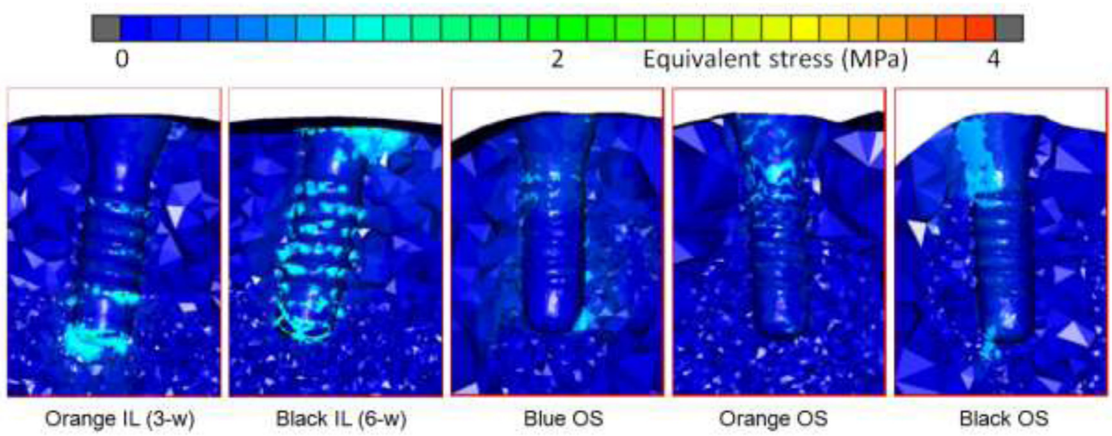

Fig. 5. Stresses distributions in the antler tissue for IL-models and OS-models. Orange IL (3-w): model of orange antler with immediately loaded implant for 3 weeks; black IL (6-w): model of black antler with immediately loaded implant for 6 weeks; blue OS: model of blue antler with unloaded implant; orange OS: model of orange antler with unloaded implant; black OS: model of black antler with unloaded implant.

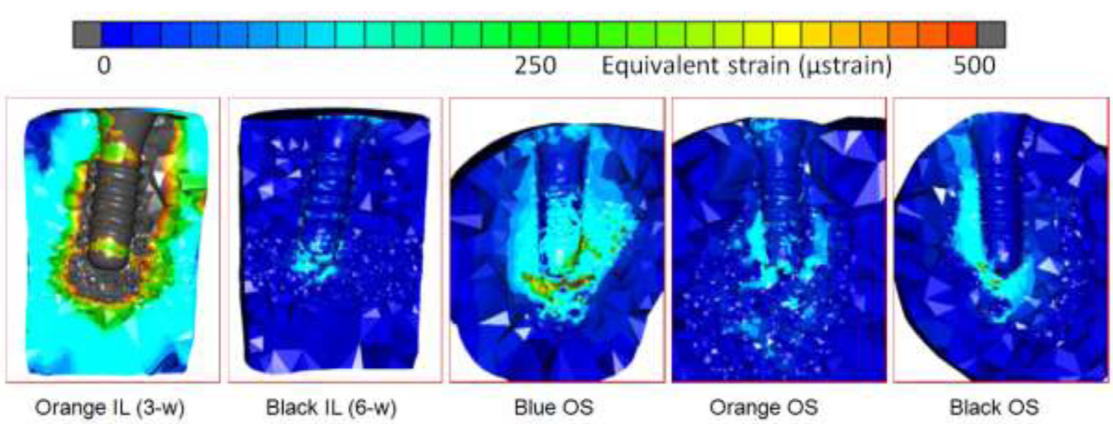

Fig. 6. Strains distributions in the antler tissue for IL-models and OS-models. Orange IL (3-w): model of orange antler with immediately loaded implant for 3 weeks; black IL (6-w): model of black antler with immediately loaded implant for 6 weeks; blue OS: model of blue antler with unloaded implant; orange OS: model of orange antler with unloaded implant; black OS: the model of black antler with unloaded implant.

Table 6
Obtained maximum values of strains (μstrain) in antler tissue in osseointegrated (OS) and immediate loading (IL) models with different postoperative time.

	IL group	OS group	*t*	*P* value
Blue (2-week)		1888 ± 171		
Orange (3-week)	9879 ± 1965	686 ± 58[a]	14.9	<0.001
Black (6-week)	363 ± 81	523 ± 48[a,b]	−5.6	<0.001
F/*t*	15.3	479.0	–	–
P value	<0.001	<0.001		

[a] $P < 0.05$, when compared with blue.
[b] $P < 0.05$, when compared with orange.

formation [23]. An optimal bone response to immediately or early loaded implants is not only determined by the primary stability of the implant and the host bone characteristics, but also by the individual loading parameters and an optimized load transfer through appropriate implant design and surface features [24,25]. In order to observe the benefit of IL implants, considerations should be made regarding the mechanical behavior of the bone under loading conditions through appropriate numerical and experimental studies for optimizing the initial stability of the implants and subsequently their long-term success.

In the present study, controlled loading was immediately applied on implants inserted into Sika deer antlers. At the same time, implants without loading were investigated as well as a control group. The results indicated that BMD and Young's modulus of antler tissue around IL implants significantly increased as the loading time increased. This is due to the reason that well-controlled IL accelerates tissue mineralization at the peri-implant bone [5]. After shedding the antler, the BMD and Young's modulus of antler tissue remained in a similar value in all specimens, including specimens with implant and specimens without implant. These values were consistent with the results of the study by Chen et al. [26], who discovered that compact bone and cancellous bone density of deer antler were 1.72 g/cm^3 and 0.50 g/cm^3 and total bone density of the antler was 1.35 g/cm^3. Moreover, the results indicated that implants inserted into Sika deer antler might not disturb the growth and calcification process of antler.

Furthermore, there was a highly interesting result that in black antler, the BMD of antler tissue around the IL implant (2.00 g/cm^3) was much higher than that around the OS implant (1.30 g/cm^3). This indicates that the density of antler tissue around the implant increases over the loading period. However the density might be reduced after the complete osseointegration of the implant as shown in previous studies [27,28].

The existing studies relating to changes in bone density around IL implants concluded various results due to the different case selection, methods of measurement, and observation times. Lahori et al. [29] evaluated the changes in periimplant bone quality for mandibular implant-supported overdentures with ball attachments using delayed and immediate loading protocols. They concluded that bone density significantly increased for both groups at all time intervals (3, 6, 12 months) and the bone density in delayed loading group illustrated higher values than that in immediate loading group. However, Hasan et al. [30] evaluated the change in bone density of 20 individual immediately loaded implants by measuring the grey values of cone beam computed tomography (CBCT) at different periods subsequent to implant insertion and observed a reduction in grey values with respect to reference values after one month and six months from implant insertion in the apical, middle, and cervical regions.

The finite element method is a numerical method which is suitable for analyzing complex structures. This method was applied mostly in biomechanical studies of dental implants and peri-implant tissues by many researchers. The validity of the simulations depends on morphology, material properties, boundary conditions, and bone-implant interface. The most important input factors are material properties of implant and surrounding tissue, such as Young's modulus and Poisson's ratio [31]. Moreover, the geometry and architecture of bone are important factors for the finite element model as well. Since the complex spongious pattern is difficult to create, spongious bone network is not considered in most FEA analyses. It was mostly assumed that spongious bone as a homogenous core surrounded by a cortical layer. Since spongious bone architecture and its density can vary among species and anatomical locations within the same individual, it is difficult to present precise results from these simplified models and validate them with clinical data. With the development of microcomputed tomography and improved performance of analytical systems, it is currently possible to conduct biomechanical analysis, taking into consideration the actual morphology and structure of spongious bone. In the present study, finite element models with spongious bone microstructure were constructed from the μCT data and Young's modulus of antler tissue was calculated from the specimens. Moreover, implants subjected to immediate loading are in frictional contact with bone, which is responsible for their primary stability. Therefore, frictional contact was simulated in this study by using a frictional contact coefficient ($\mu = 0.3$) at the bone-implant interface [32,33]. Osseointegrated condition was simulated by defining perfect bonding interface between the bone and implant [34]. The above mentioned methods enabled the models to imitate the real situation as much as possible.

The results of this study showed that the maximum values of displacement and stress in implant and stress and strain in antler tissue were significantly different among OS models. This might be attributed to the various densities and geometries of antler tissue in different animals. In OS models with higher BMD and Young's modulus, strains in antler tissue were lower. This is due to the reason that the deformation of the bone tissue by means of strain is inversely correlated to its stiffness. The higher the strain value, the lower the stiffness of the bone.

Comparing the orange antler models, all the biomechanical results of IL model were significantly higher than those of orange antler OS model ($P < 0.05$) and wider distributions were obtained from IL models. Conversely, for black antler models, the displacements in implant and strains in antler tissue of IL model were significantly lower than OS model ($P < 0.05$) and narrower distribution of strains were detected in IL model. Theoretically, IL models should indicate higher biomechanical results, because only compressive and frictional forces are transferred via the contacting interfaces, compared with the bonded interfaces of the OS models. However, the models constructed in this study were from various specimens, and the biomechanical values can be influenced by the density of antler tissue, the geometry of antler tissue and contact condition of bone-implant interface. The considerably higher density of antler tissue in black antler IL model might be a reason for these results.

There were limitations in this study. First, the limited numbers of animal specimens, only three pairs of antlers were collected after their shedding due to the fact that it was difficult to find all the shedded antlers in a spacious activity place for Sika deer. Secondly, an empirical equation was used to calculate Young's modulus of antler tissue from BMD. However, this study provided theoretical foundation for developing the deer antler as a novel model for dental implant investigation.

5. Conclusions

After shedding the antler, the BMD of antler tissue in specimens with osseointegrated implants and without implants remained in a similar range. Implants inserted into Sika deer antler do not disturb the growth and calcification process of antler.

Density of antler tissue around the implant go up to relatively higher values after under immediate loading for a longer time period and the density might be reduced after osseointegration of the implant.

The biomechanical values are influenced by the density of antler tissue, the geometry of antler tissue and contact conditions of the bone-implant interface.

Funding

This investigation was supported by Straumann GmbH (Freiburg, Germany) and grants from National Natural Science Foundation of China (11702231). The study sponsors have no involvement in the study design, in the collection, analysis and interpretation of data, in the writing of the manuscript, or in the decision to submit the manuscript for publication.

Conflict of interest

The authors declare that there is no conflict of interest.

Acknowledgments

The authors thank the staff of Raptor Center and Wildlife Parc Hellenthal, especially Mr. Joerg Niesters, Mr. Karl Fischer, Mr. Dirk Wynands and Dr. Martin Boettcher for care of the animals, thank the staff of Endowed Chair of Oral Technology, University of Bonn, Dr. Susanne Reimann and Ms. Anna Weber for preparing and scanning the specimens by µCT scanner, and thank Mr. Tim Klunter for taking out the specimens from antlers.

References

[1] Albrektsson T, Brånemark PI, Hansson HA, Lindström J. Osseointegrated titanium implants. Requirements for ensuring a long-lasting, direct bone-implant anchorage in man. Acta Orthop Scand 1981;52:155–70.
[2] Albrektsson T, Johansson C. Osteoinduction, osteoconduction andosseointegration. Eur Spine J 2001;10(Suppl 2):S96–S101.
[3] Joos U, Meyer U. New paradigm in implant osseointegration. Head FaceMed 2006;2:19.
[4] Camargos GV, Sotto-Maior BS, Silva WJ, Lazari PC, Del Bel Cury AA. Prosthetic abutment influences bone biomechanical behavior of immediately loaded implants. Braz Oral Res 2016;30:1–9.
[5] Duyck J, Vandamme K. The effect of loading on peri-implant bone: a critical review of the literature. J Oral Rehabil 2014;41:783–94.
[6] Romanos GE. Biomolecular cell-signaling mechanisms and dental implants: a review on the regulatory molecular biologic patterns under functional and immediate loading. Int J Oral Maxillofac Implants 2016;31:939–51.
[7] Melilli D, Rallo A, Cassaro A. Implant overdentures: recommendations and analysis of the clinical benefits. Minerva Stomatol 2011;60:251–69.
[8] Pearce AI, Richards RG, Milz S, Schneider E, Pearce SG. Animal models for implant biomaterial research in bone: a review. Eur Cell Mater 2007;13:1–10.
[9] Schimandle JH, Boden SD. Spine update. The use of animal models to study spinal fusion. Spine 1994;19:1998–2006.
[10] Li C, Zhao H, Liu Z, McMahon C. Deer antler-a novel model for studying organ regeneration in mammals. Int J Biochem Cell Biol 2014;56:111–22.
[11] Goss RJ. Future directions in antler research. Anat Rec 1995;241:291–302.
[12] Li C, Suttie JM. Tissue collection methods for antler research. Eur J Morphol 2003;41:23–30.
[13] Currey JD, Landete-Castillejos T, Estevez J, Ceacero F, Olguin A, Garcia A, Gallego L. The mechanical properties of red deer antler bone when used in fighting. J Exp Biol 2009;212:3985–93.
[14] Rolf HJ, Enderle A. Hard fallow deer antler: a living bone till antler casting? Anat Rec 1999;255:69–77.
[15] Kierdorf U, Stoffels E, Stoffels D, Kierdorf H, Szuwart T, Clemen G. Histological studies of bone formation during pedicle restoration and early antler regeneration in roe deer and fallow deer. Anat Rec A Discov Mol Cell Evol Biol 2003;273:741–51.
[16] Li C, Suttie JM, Clark DE. Histological examination of antler regeneration in red deer (Cervus elaphus). Anat Rec A Discov Mol Cell Evol Biol 2005;282:163–74.
[17] Caulkett N, Haigh JC. Deer (Cervids). In: West G, Heard D, Caulkett N, editors. Zoo animal and wildlife immobilization and anaesthesia. Ames Iowa: Blackwell Publishing; 2007. p. 607–12.
[18] Wiesner H, von Hegel G. Practical advice concerning the immobilization of wild and zoo animals. Tierarztl Prax 1985;13:113–27.
[19] Rahimi A, Klein R, Keilig L, Abboud M, Wahl G, Bourauel C. Development and design of a novel loading device for the investigation of bone adaptation around immediately loaded dental implants using the reindeer antler as implant bed. J Biomech 2009;42:2415–18.
[20] Beaupré GS, Orr TE, Carter DR. An approach for time-dependent bone modeling and remodeling-theoretical development. J Orthop Res 1990;8:651–61.
[21] Gottlow J, Dard M, Kjellson F, Obrecht M, Sennerby L. Evaluation of a new titanium-zirconium dental implant: a biomechanical and histological comparative study in the mini pig. Clin Implant Dent Relat Res 2012;14:538–45.
[22] Webster D, Schulte FA, Lambers FM, Kuhn G, Müller R. Strain energy density gradients in bone marrow predict osteoblast and osteoclast activity: a finite element study. J Biomech 2015;48:866–74.
[23] Balaji P, Balaji SM, Ugandhar P. Immediate implant in single rooted teeth – study on primary stability and bone formation. Indian J Dent Res 2015;26:421–6.
[24] Götz W, Gedrange T, Bourauel C, Hasan I. Clinical, biomechanical and biological aspects of immediately loaded dental implants: a critical review of the literature. Biomed Techol 2010;55:311–15.
[25] Schnitman PA, Hwang JW. To immediately load, expose, or submerge in partial edentulism: a study of primary stability and treatment outcome. Int J Oral Maxillofac Implants 2011;26:850–9.
[26] Chen PY, Stokes AG, McKittrick J. Comparison of the structure and mechanical properties of bovine femur bone and antler of the North American elk (Cervus elaphus canadensis). Acta Biomater 2009;5:693–706.
[27] Ramachandran A, Singh K, Rao J, Mishra N, Jurel SK, Agrawal KK. Changes in alveolar bone density around immediate functionally and nonfunctionally loaded implants. J Prosthet Dent 2016;115:712–17.
[28] Mainetti T, Lang NP, Bengazi F, Sbricoli L, Soto Cantero L, Botticelli D. Immediate loading of implants installed in a healed alveolar bony ridge or immediately after tooth extraction: an experimental study in dogs. Clin Oral Implants Res 2015;26:435–41.
[29] Lahori M, Kaul AS, Chandra S, Nagrath R, Gupta H. Comparative evaluation of bone in mandibular implant retained overdentures using delayed and immediate loading protocol: an in-vivo study. J Indian Prosthodont Soc 2013;13:113–21.
[30] Hasan I, Dominiak M, Blaszczyszyn A, Bourauel C, Gedrange T, Heinemann F. Radiographic evaluation of bone density around immediately loaded implants. Ann Anat 2015;199:52–7.
[31] Seker E, Ulusoy M, Ozan O, DÖ Doğan, Seker BK. Biomechanical effects of different fixed partial denture designs planned on bicortically anchored short, graft-supported long, or 45-degree-inclined long implants in the posterior maxilla: a three-dimensional finite element analysis. Int J Oral Maxillofac Implants 2014;29:e1–9.
[32] Hasan I, Keilig L, Staat M, Wahl G, Bourauel C. Determination of the frictional coefficient of the implant-antler interface: experimental approach. Biomed Technol 2012;57:359–63.
[33] Huang HL, Hsu JT, Fuh LJ, Tu MG, Ko CC, Shen YW. Bone stress and interfacial sliding analysis of implant designs on an immediately loaded maxillary implant: a non-linear finite element study. J Dent 2008;36:409–17.
[34] Murakami N, Wakabayashi N. Finite element contact analysis as a critical technique in dental biomechanics: a review. J Prosthodont Res 2014;58:92–101.

3.3 Study 3

Numerical Investigation of Bone Remodelling Around Immediately Loaded Dental Implants Using Sika Deer (Cervus nippon) Antlers as Implant Bed

Yun He, Istabrak Hasan, Ludger Keilig, Dominik Fischer, Luisa Ziegler, Markus Abboud, Gerhard Wahl, Christoph Bourauel

Computer Methods in Biomechanics and Biomedical Engineering 2018; 21: 359-369
doi: 10.1080/10255842.2018.1462346
Impact Factor ^{2017}: 1.974

COMPUTER METHODS IN BIOMECHANICS AND BIOMEDICAL ENGINEERING, 2018
VOL. 21, NO. 4, 359–369
https://doi.org/10.1080/10255842.2018.1462346

Taylor & Francis
Taylor & Francis Group

Check for updates

Numerical investigation of bone remodelling around immediately loaded dental implants using sika deer (Cervus nippon) antlers as implant bed

Yun He[a], Istabrak Hasan[b], Ludger Keilig[c], Dominik Fischer[d], Luisa Ziegler[d], Marcus Abboud[e], Gerhard Wahl[f] and Christoph Bourauel[c]

[a]Orofacial Reconstruction and Regeneration Laboratory, Department of Oral and Maxillofacial Surgery, The Hospital of Stomatology, Southwest Medical University, Luzhou, China; [b]Department of Prosthetic Dentistry, Preclinical Education and Materials Science, Dental School, Rheinische Friedrich Wilhelms Universitat Bonn, Endowed Chair of Oral Technology, Bonn, Germany; [c]Oral Technology, University of Bonn, Bonn, Germany; [d]Clinic for Birds, Reptiles, Amphibians and Fish, Veterinary Faculty, Justus Liebig University Giessen, Giessen, Germany; [e]Department of Prosthodontics and Digital Technology, School of Dental Medicine, Stony Brook University, New York, NY, USA; [f]Department of Oral Surgery, Dental School, University of Bonn, Bonn, Germany

ABSTRACT

This study combines finite element method and animal studies, aiming to investigate tissue remodelling processes around dental implants inserted into sika deer antler and to develop an alternative animal consuming model for studying bone remodelling around implants. Implants were inserted in the antlers and loaded immediately via a self-developed loading device. After 3, 4, 5 and 6 weeks, implants and surrounding tissue were taken out. Specimens were scanned by µCT scanner and finite element models were generated. Immediate loading and osseointegration conditions were simulated at the implant-tissue interface. A vertical force of 10 N was applied on the implant. During the healing time, density and Young's modulus of antler tissue around the implant increased significantly. For each time point, the values of displacement, stresses and strains in the osseointegration model were lower than those of the immediate loading model. As the healing time increased, the displacement of implants was reduced. The 3-week immediate loading model (9878 ± 1965 µstrain) illustrated the highest strains in the antler tissue. Antler tissue showed similar biomechanical properties as human bone in investigating the bone remodelling around implants, therefore the use of sika deer antler model is a promising alternative in implant biomechanical studies.

ARTICLE HISTORY
Received 2 October 2017
Accepted 4 April 2018

KEYWORDS
Implant; sika deer antler; immediate loading; bone mineral density

1. Introduction

Dental implantology is a widely-used and well-established therapy for a large number of cases of lost teeth. Integration of implant anchored or implant supported reconstructions of the masticatory apparatus is a good approximation to the ideal case of function (Bassi et al. 2013; Boven et al. 2015). Currently immediately loaded implants (one-stage technique) are an emerging treatment alternative that may be described as functional loading immediately after implantation without waiting for a healing period (Barndt et al. 2015; Al-Sawai and Labib 2016). In contrast, the conventional protocol advocates a two-stage technique with a load-free healing phase for three to six months (Albrektsson et al. 1981; Brånemark 1983).

Apparently, immediate loading (IL) of implants increases implant acceptability by reducing treatment time and providing both, physical and psychological benefits to patients. Accordingly, in several animal experimental studies, such as dogs (Huang et al. 2015; Mainetti et al. 2015; Simion et al. 2015), rabbits (Vandamme et al. 2007; Kunnekel et al. 2011; Han et al. 2014) or rats (Matin et al. 2003; Sato et al. 2014) bone remodelling processes with respect to IL around implants have been investigated. The results indicated that IL had a positive effect on the tissue differentiation and bone formation around titanium implants, and IL significantly increased bone stress during the early postoperative period. However, these animal experiments are problematic due to different reasons. Firstly, the investigation commonly causes an enormous stress due to repeated anesthetisation and surgery of the animals in order to realise a controlled loading protocol. Secondly, the load applied on endosseous implants is difficult to control, because the loading device in the mouth or on top of other bone sites might be affected by many

CONTACT Istabrak Hasan ihasan@uni-bonn.de

© 2018 Informa UK Limited, trading as Taylor & Francis Group

factors, such as food intake and physiologic activity. Last but not least, the fortune of the animals is sacrifice.

The use of antlers in a new animal model - the sika deer (Cervus nippon) - offers the possibility to study the remodelling process around implants in multiple times without sacrificing the animal. The antler of deer is the only mammalian organ that can fully grow back once lost from its pedicle, the base from which it re-grows each summer after shedding it in spring annually. This annually growth is very fast rate and completes in just three to four months (Chen et al. 2009). This allows carrying out investigations of immediately loaded dental implants in a relatively acceptable time span without affecting the maturation of the future antlers. Being sensitive to manipulation during growth, antlers are barely sensitive when growth is completed, as they are intended to be used as weapons to fight against conspecifics. This enables also to place implants over a prolonged time in the antlers and to retrieve them when antlers are regularly shed by the deer. Furthermore, deer antlers with high collagen content and the ability to bear tensile and compressive forces in their normal functional state have similar elastic and fracture behaviour to that of human bone (Currey et al. 2009). Finally, sika deer are very tame, easy to handle and to breed.

The finite element method (FEM) plays an important role in solving engineering problems in many fields of science. The FEM can successfully be applied in simulations of biomechanical systems, e.g. for studying the biomechanical parameters in peri-implant bone. It allows taking into consideration the key features, like material mechanical properties as well as the very complicated geometry of biological structures. The very dynamic temporal change in bone structure by healing and bone remodelling cannot directly on the technical side be detected, neither by experimental methods nor using standard finite element methods. With respect to IL dental implants in particular, there is as yet no clear correlation of mechanical parameters and biological reactions. In view of this, this study combines FEM and animal experimental studies, aiming to investigate the tissue remodelling process around implants inserted into sika deer antler under IL condition. Furthermore, the aim was to develop an alternative animal model for studying bone remodelling around dental implants without requiring euthanasia of animals.

2. Methods

2.1. Loading device

The autonomous loading device used in the animal trial was custom-made and designed for antlers (Rahimi et al. 2009). Briefly, this unit was able to apply a maximum load of 100 N with a power supply of 12 V. Purely vertical loads were produced by using a spherical head of the implant abutment.

2.2. Placements of implants in sika deer antler

In this study all animals were handled according to the policies and principles established by the German animal welfare act (TSchG, lastly amended on 3rd December 2015), approved by the North Rhine-Westphalia State Agency for Nature, Environment and Consumer Protection as competent authority (Permission No.: LANUV NRW, 84-02.04.2014.A462). Straumann Roxolid® soft tissue level implants (Institut Straumann AG, Basel, Switzerland) with a length of 10 mm and a diameter of 3.3 mm were used. Six 4 years old male sika deer (bred at Wildlife Parc Hellenthal) were anesthetized using 1.2–1.5 ml Hellabrunn's Mixture (100 mg Ketamine & 125 mg Xylazine per ml) using distance immobilization darts shot from a carbon-dioxide-injection gun (DAN-INJECT JM Standard injection rifle, DAN-INJECT Smith GmbH, Walsrode, Germany) according to standard procedures (Caulkett and Haigh 2007; Wiesner and von Hegel 1985). After disinfection with 70% alcohol and 1% iodine tincture (Applichen GmbH, Darmstadt, Germany) and additional local anaesthesia with 3–5 ml lidocaine (Lidocain B. Braun 2%, B. Braun Melsungen, Melsungen, Germany), a longitudinal cut was performed and velvet flap elevated. Implant site at a position near a branching of the antler was prepared by sequential drilling under sterile saline irrigation according to the surgical protocol. Two implants per antler were inserted in a distance of 2.5 cm. The most proximal implant was vertically loaded immediately via the self-developed screw retained loading device (Rahimi et al. 2009), while the other one remained unloaded as a control (Figure 1). One deer was dead during the anesthetization phase due to severe complication. Postoperatively, animals and wounds of the five animals were inspected daily for the absence of wound healing complications, alteration of general health, abnormal behavior and reduced food uptake and the loading devices were checked visually. After 2, 3, 4, 5 and 6 weeks, respectively, the loaded implants and surrounding tissue were randomly taken out with a trephine from one animal and the wounds were filled with bone wax ((Ethicon®-bone wax, Johnson and Johnson, Hamburg, Germany)), sutured and bandage protected. The samples were fixed in buffered formalin (4%). The unloaded implants were remained in the antler for further osseointegration investigation.

2.3. Numerical analysis

As the sample of 2-week was not suitable for μCT scanning, it was directly sent for histological analysis. Then,

Figure 1. Insertion of a dental implant into the sika deer antler (left).
Notes: Each animal receives two implants at a position near a branching of the antler. One of the implants is loaded by an autonomous loading device, controlled by a micro-computer. The implant is loaded by a motor driven thrust die (arrow in the figure on the right).

four specimens were prepared and scanned in a µCT scanner (SkyScan 1174, Bruker-microCT, Kontich, Belgium) using 50 kV and 800 µA, rotation step 0.25°. A 1 mm thick aluminum filter was used for beam-hardening reduction. The exposure time was set at 2 s. Scan times were approximately ten hours per sample. Datasets were reconstructed. After scanning the sample, the calibration phantom with known density of calcium hydroxyapatite (SkyScan 1174, Bruker-microCT, Kontich, Belgium) was scanned on the same day by using the same parameters. Bone mineral density (BMD) of antler tissue was calculated by using Bruker-MicroCT CT-Analyser (Bruker-microCT, Kontich, Belgium).

µCT data were imported into Mimics research 17.0 (Materialise NV, Leuven, Belgium). Later on, two masks were created by defining different Hounsfield range, including the mask of implant, antler tissue. Using the option of '3D reconstruction' the masks were reconstructed, and further processed in 3-Matic research 9.0 (Materialise NV, Leuven, Belgium). Due to the requirements of the µCT scanner, the antler tissue around the implant in the samples was reduced and not sufficient for FEA. In order to imitate the real situation in live antler and keep the sample as the similar size for reasonable comparison (at least 5 mm thickness of the antler tissue around the implant), antler tissue around the implant was expanded to the same geometry by importing data of the antler tissue without implant (Figure 2). Thereafter, the models were converted into 3D FE models using 4-noded tetrahedral elements. The final models consisted of 243,009; 258,158; 235,297; and 244,003 elements in 3, 4, 5 and 6 weeks respectively. 3D FE analysis was performed using the software package MSC.Marc/Mentat 2010 (MSC. Software, Santa Ana, CA, U.S.A.).

All materials were assumed to be homogenous, isotropic and linear elastic. Young's modulus of the antler tissue was calculated by using the formula (Beaupré et al. 1990):

$$E = \begin{cases} 2014\rho^{2.5} & \text{if } \rho \leq 1.25 \text{ g/cm}^3 \\ 1763\rho^{3.2} & \text{if } \rho > 1.25 \text{ g/cm}^3 \end{cases}$$

Material properties of the implant (Roxolid® material) and bone marrow that were used in the analysis were taken from the literature (Table 2) (Gottlow et al. 2012; Webster et al. 2015).

Two conditions were investigated at the implant-tissue interface, IL and osseointegration (OS). As for IL condition, a friction contact (friction coefficient 0.3) was defined between the implant and antler tissue (Beaupré et al. 1990).

All models were constrained in all directions at the nodes on the mesial, distal and bottom of the antler tissue. For comparison reasons, a vertical force of 10 N was applied on the implant. Displacements, stresses and strains were evaluated and compared for all models. The mean values were recorded and presented as mean ± standard deviation (SD).

2.4. Statistic evaluation

As for the maximum values of displacements and stresses in the implant as well as stresses and strains in antler tissue, data were analysed using IBM SPSS Statistics for Windows, version 20.0 software (IBM Corp., Armonk, NY, U.S.A.). Factorial design ANOVA was used to evaluate the effect of time and contact condition. Time consisted of four levels (3, 4, 5, 6 weeks) and the contact condition included two levels (IL and OS). If a significant time by contact condition interaction was found, the values at the same time point were compared using one-way ANOVA with the SNK comparison test. A significance level of 0.05 was chosen.

Null hypothesis were:

(1) There is a significant difference in bone density in different time points.

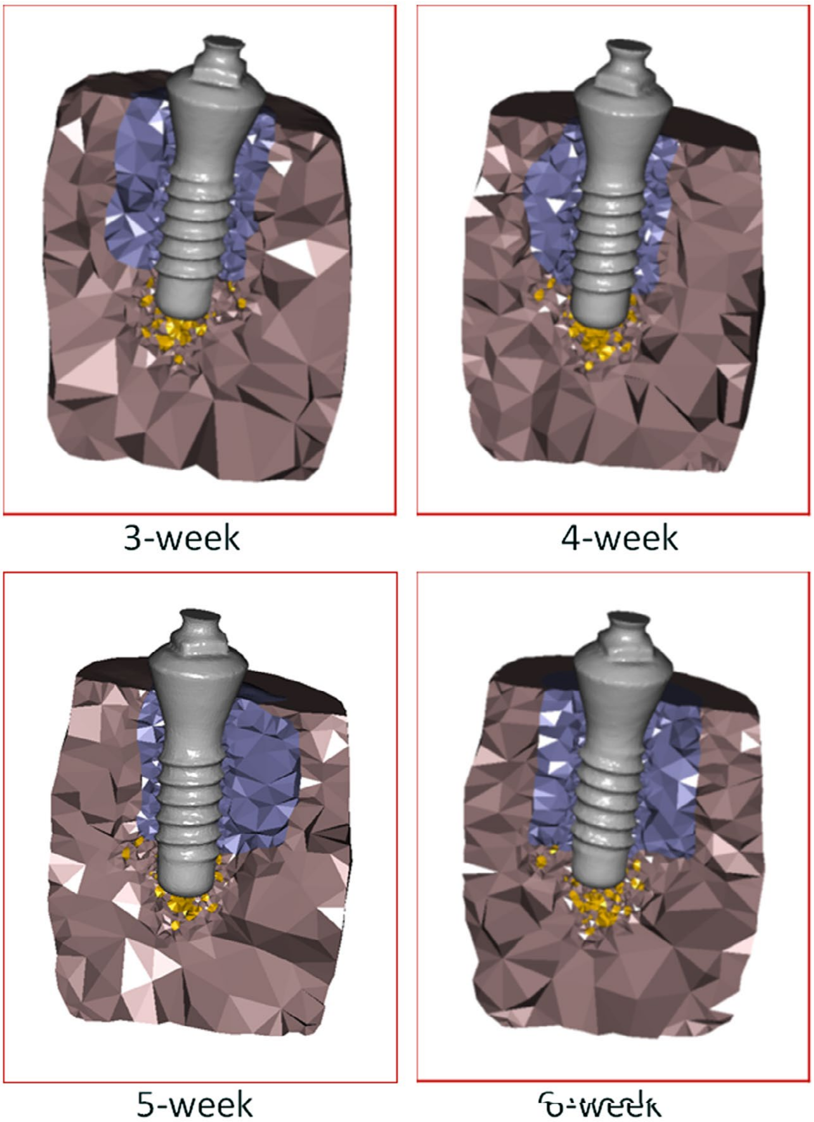

Figure 2. Finite element model of sika deer antler after inserting implant 3, 4, 5, 6 weeks.
Notes: Grey: implant, blue: original antler tissue around the implant in the samples, Brown: expanded antler tissue, yellow: bone marrow.

(2) There is a significant reduction of implant displacement in both OS and IL conditions, after 3, 4, 5, 6 weeks from implantation.
(3) There is a significant reduction of implant stress in both OS and IL conditions, after 3, 4, 5, 6 weeks from implantation.
(4) There is a significant increase in stresses of antler tissue in both OS and IL conditions, after 3, 4, 5, 6 weeks from implantation.
(5) There is a significant reduction of strains in antler tissue in both OS and IL conditions, after 3, 4, 5, 6 weeks from implantation.
(6) There is a significant reduction of displacements and stresses in implant, stresses and strains in antler tissue in OS condition in comparison to IL condition at the same time point.

3. Results

3.1. Animal health and behaviour after implantation and loading

Five animals are in good conditions. No signs of infections or other complications occurred during the postoperative phase. Sutures were removed after 1-week healing period, without any inflammation. No altered behaviours of the sika deer and the growth of antlers were observed.

3.2. BMD and Young's Modulus of the antler tissue

During the healing time after insertion of the implant, BMD and Young's Modulus of the antler tissue around the implant increased significantly (Table 1). After 6 weeks, the values (2.00 ± 0.53 g/cm^3 and 16,200 ± 230 MPa) were

Table 1. BMD and Young's Modulus of the antler tissue around implants at different healing periods.

Time	BMD (g/cm^3)	Young's Modulus (MPa)
3-week	0.31 ± 0.01	107.76 ± 0.02
4-week	0.92 ± 0.23	1,635 ± 51
5-week	1.54 ± 0.40	6,591 ± 94
6-week	2.00 ± 0.53	16,200 ± 230

Table 2. Material properties of numerical models.

Material	Young's Modulus (MPa)	Poisson ratio
Roxolid®	98,000	0.30
Bone marrow	2	0.16
Antler tissue (3-week)	108	0.30
Antler tissue (4-week)	1,635	0.30
Antler tissue (5-week)	6,591	0.30
Antler tissue (6-week)	16,200	0.30

similar to that of human cortical bone (Tassani et al. 2011). The corresponding material properties of the numerical models were shown in Table 2.

3.3. FE results

The results of factorial design ANOVA for the maximum values of stresses in the implant as well as stresses and strains in the antler tissue showed the effect of time, contact condition and the interaction between time and contact condition to be statistically significant ($P < .05$). Therefore, the different contact conditions at the same time point were compared. For each time point, the values of displacement, stresses and strains in the OS model were noticeably lower than that of the IL model ($P < .05$).

As the healing time increased, the displacement of the implant was reduced (Table 3). The differences were significant except between 5-week and 6-week for OS models, no significant difference was observed. The highest values of the maximum displacement of implant (6.2 ± 0.3 µm) were observed with 3-week IL model. The 6-week OS models showed the lowest values of the maximum displacement of the implant (0.3 ± 0.1 µm).

Stresses in the implant were significantly decreased and concentrated in small area while the healing time was increasing. All IL models showed higher values compared to OS models at the same time point (Table 4, Figure 3), and the values had significant differences ($P < .05$) except for 3-week models. The lowest and highest values of stresses in implants were obtained in 6-week OS model (1.5 ± 0.1 MPa) and 3-week IL model (2.8 ± 0.1 MPa).

Stresses in antler tissue were increased during the healing time. In 5-week and 6-week IL models, the antler tissue around the neck, screws and tip of the implant indicated higher stresses (6.5 ± 2.8 Mpa and 6.5 ± 1.6 MPa) and wider distribution compared to other models. The

Table 3. Obtained maximum values of displacements in implant (µm) in immediate loading (IL) and osseointegration (OS) models with different postoperative time.

	IL group	OS group	*t*	*P* value
3-week	6.2 ± 0.3	3.9 ± 0.2	−19.3	<.001
4-week	1.7 ± 0.1[a]	1.5 ± 0.1[a]	−3.5	=.002
5-week	0.7 ± 0.1[ab]	0.4 ± 0.1[ab]	−7.7	<.001
6-week	0.4 ± 0.1[abc]	0.3 ± 0.1[ab]	−3.1	=.007
F	2453.7	1355.4	–	–
P value	<.001	<.001		

Notes: [a]$P < .05$, when compared with 3-week group.
[b]$P < .05$, when compared with 4-week group.
[c]$P < .05$, when compared with 5-week group.

Table 4. Obtained maximum values of stresses in implant (MPa) in immediate loading (IL) and osseointegration (OS) models with different postoperative time.

	IL group	OS group	t	*P* value
3-week	2.8 ± 0.1	2.8 ± 0.1	−1.2	=.27
4-week	2.8 ± 0.2	2.5 ± 0.1[a]	−4.0	=.001
5-week	2.5 ± 0.1[ab]	2.0 ± 0.1[ab]	−8.0	<.001
6-week	2.5 ± 0.0[ab]	1.5 ± 0.1[abc]	−25.3	<.001
F	21.7	286.0	–	–
P value	<.001	<.001		

Notes: [a]$P < .05$, when compared with 3-week group.
[b]$P < .05$, when compared with 4-week group.
[c]$P < .05$, when compared with 5-week group.

values were almost three times as large as that of 3-week IL model (Table 5, Figure 4). The lowest values were obtained in the 3-week OS model (0.7 ± 0.2 MPa).

Strains in antler tissue were significantly reduced during the healing time (Table 6, Figure 5). The values of strains in antler tissue with the OS model were dramatically lower than that of the IL model at each time point, and there were significant differences between them ($P < .05$). The 6-week OS model (49 ± 7 µstrain) and the 3-week IL model (9878 ± 1965 µstrain) illustrated the lowest and highest values of maximum strains in the antler tissue.

4. Discussion

Presently, there is an increasing interest to immediate or early loaded implants, because it considerably shortens the treatment duration and reduces the number of surgeries. Clinical studies have documented satisfactory survival rate of IL implants (Testori et al. 2004; Esposito et al. 2016). However, it is indicated that the failure rate is relatively high when the conditions of the recipient site are compromised (Lekholm 2003; Zuffetti et al. 2016), and when the implant is placed at a high loading region, such as a molar site (Romanos and Nentwig 2006; Torroella-Saura et al. 2015). It is necessary to analyse intensively into if early loading is the direct reason for the failure of immediate loading implant. However, many factors,

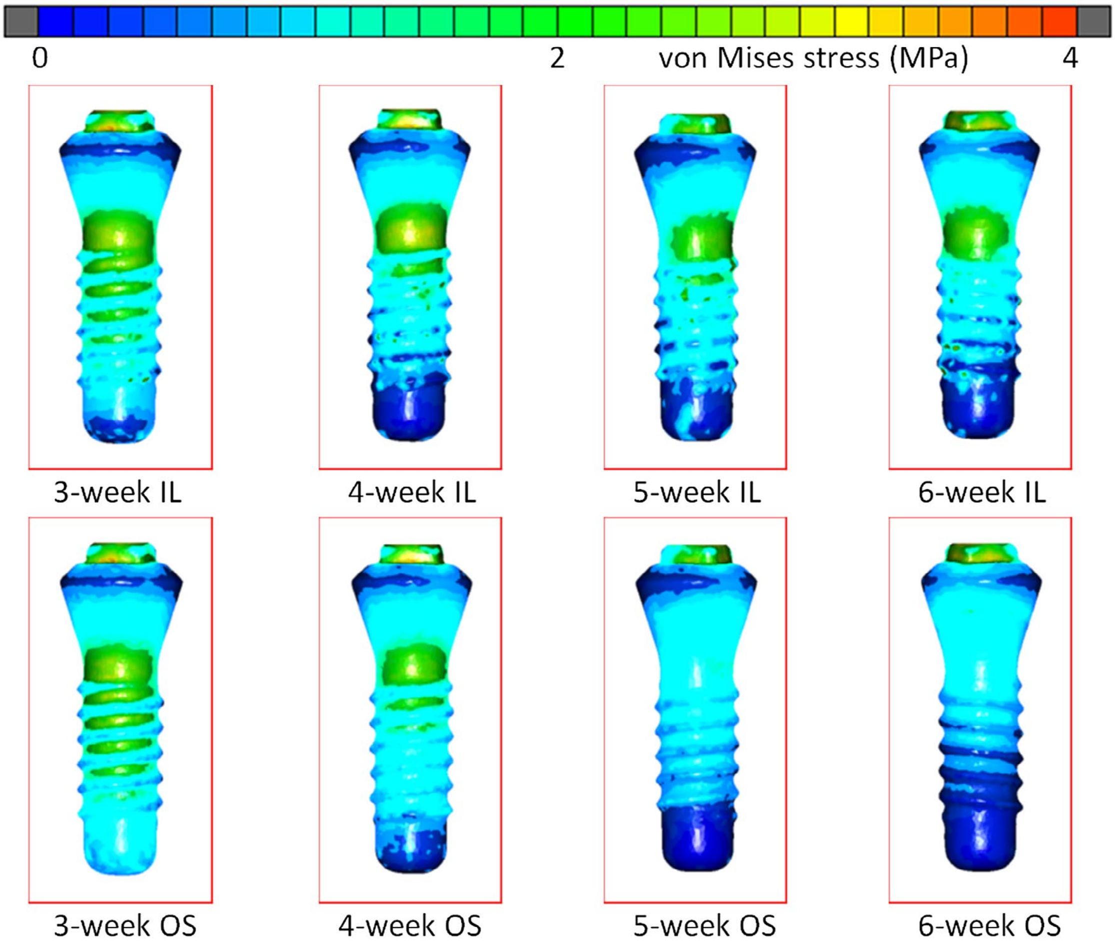

Figure 3. Comparison of the stresses in implant.
Notes: From above to below: immediate loading (IL) and osseointegration (OS) models. From left to right, models in 3, 4, 5, 6 weeks.

Table 5. Obtained maximum values of stresses in antler tissue (MPa) in osseointegration (OS) and immediate loading (IL) models with different postoperative time.

	IL group	OS group	t	*P* value
3-week	2.4 ± 0.8	0.7 ± 0.2	−7.2	<.001
4-week	3.0 ± 0.6	0.8 ± 0.2	−12.6	<.001
5-week	6.5 ± 2.8^{ab}	1.6 ± 0.7^{ab}	−5.3	<.001
6-week	6.5 ± 1.5^{ab}	1.7 ± 0.3^{ab}	−9.7	<.001
F	17.1	17.8	–	–
P value	<.001	<.001		

Notes: $^{a}p < 0.05$, when compared with 3-week group.
$^{b}p < 0.05$, when compared with 4-week group.

such as food intake, oral environment and physiological activities, make it difficult to control the loading on the implant. The traditional research methods cannot solve this problem. It was important in the present study to exclude other interfering factors by using deer antler as an implant bed with a controlled loading device. During the experiment, it was observed a normal behaviour of deer and antler regeneration was not disturbed, and the deer physiological behaviour did not affect our loading trial. Therefore, antlers can be safely and effectively used as a novel method for implantation research.

A successful dental implant treatment relies on maintaining the stability of the implant within the host bone site. This condition is achieved through osseointegration, which consists of healing and remodelling phases (Brånemark 1983). Bone is capable of adapting to its mechanical environment by changing its density and internal micro-architectural organization according to the magnitude and directionality of the applied external forces. This remarkable ability for adapting to loading is thought to be a result of the orchestrated action of bone cells in an on-going process called bone remodelling, where bone is added at high-load locations and removed at low-load locations (‘Wolff’s law’) (Frost 2004). Imaging, resonance frequency and histological evaluation have documented the effect (Duyck et al. 2001; Gotfredsen et al. 2002; De Smet et al. 2006; Granić et al. 2015) of loading on bone response around the implant, but the real biomechanical environment in peri-implant bone and the subsequent bone response have not been

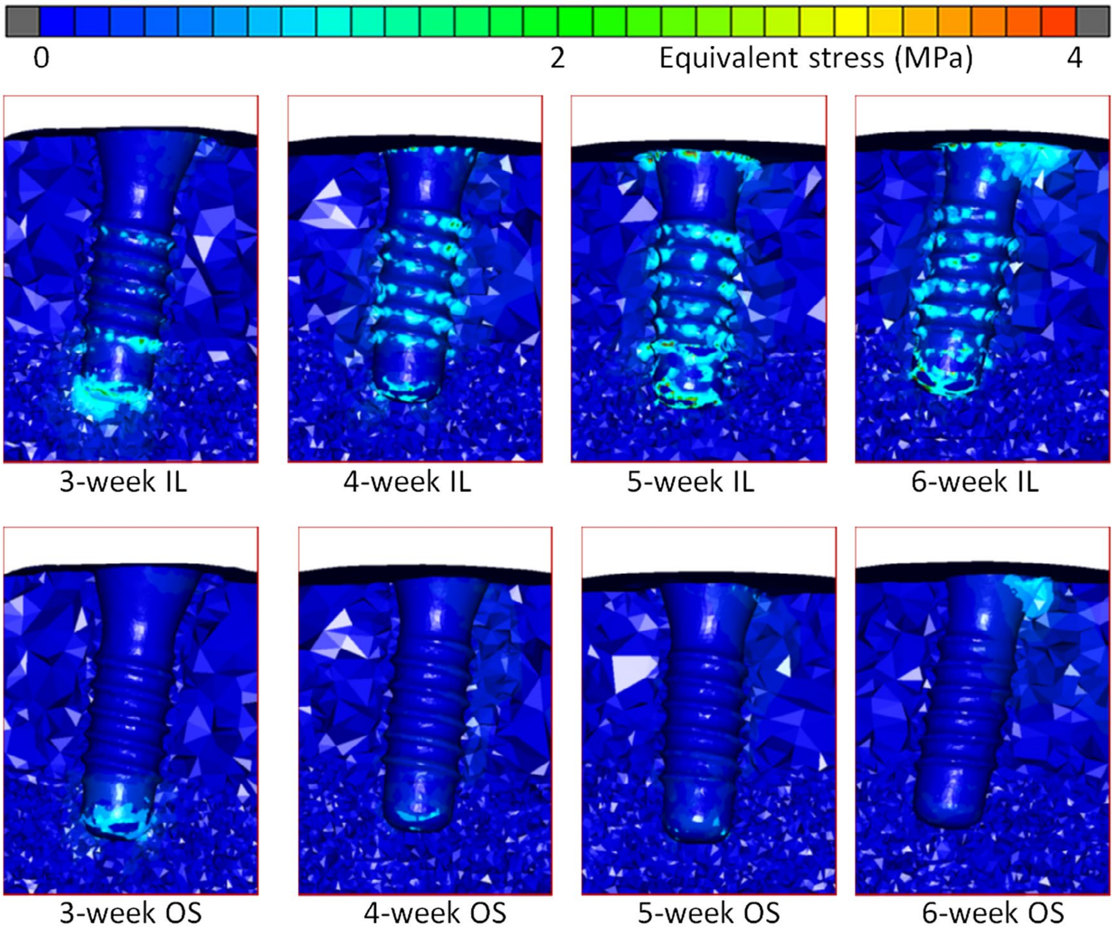

Figure 4. Comparison of the stresses in antler tissue.
Notes: From above to below: immediate loading (IL) and osseointegration (OS) models. From left to right, models in 3, 4, 5, 6 weeks.

Table 6. Obtained maximum values of strains in antler tissue (μstrain) in osseointegration (OS) and immediate loading (IL) models with different postoperative time.

	IL group	OS group	t	*P* value
3-week	9879 ± 1965	2608 ± 892	−10.7	<.001
4-week	2188 ± 386[a]	879 ± 324[a]	−8.2	<.001
5-week	1260 ± 329[ab]	172 ± 60[ab]	−10.3	<.001
6-week	363 ± 81[ab]	49 ± 8[ab]	−12.2	<.001
F	185.0	61.5	–	–
P value	<.001	<.001		

Notes: [a]$P < .05$, when compared with 3-week group.
[b]$P < .05$, when compared with 4-week group.

adequately explained during the osseointegration process, due to *in vivo* measurement limitations. A thorough understanding of the early osseointegration phases could provide an additional basis to support the extended use of IL therapy.

Therefore, the aim of this study was to use a novel animal model for evaluating the bone remodelling around IL implants during the healing time. To our knowledge, this is the first time to use deer antler as an implant bed with a controlled loading device. The main advantage of using sika deer antlers as a novel animal model is mainly related to the opportunity of having the antler samples without the need of animal sacrificing, which is associated with all established animal experiments. Besides, in this study, we used μCT data of the antler samples to reconstruct the real condition, and calculate the BMD and Young's modulus from the sample.

It is reported that mammals and humans have similar biological responses to mechanical stimuli and the biomechanical properties of deer antler is somehow similar to that of human bone (Currey et al. 2009; Launey et al. 2010). Currey et al. (2009) experimentally measured Young's modulus for the red deer (Cervus elaphus) antler in wet and dry conditions (wet: 7.30 GPa, dry: 17.50 GPa). Paramio et al. (2012) found the density of red deer antler by the hydrostatic method was 1.112 ± 0.120 g/cm^3 and 1.112 ± 0.158 g/cm^3 by the 3D-CAD method. Compared to abovementioned studies, the material characteristics of the antler tissue in the present study was relatively low in the early postoperative period, but the density and Young's Modulus increased during the healing time and reach 2.00 ± 0.53 g/cm^3 and 16,200 ± 230 MPa after

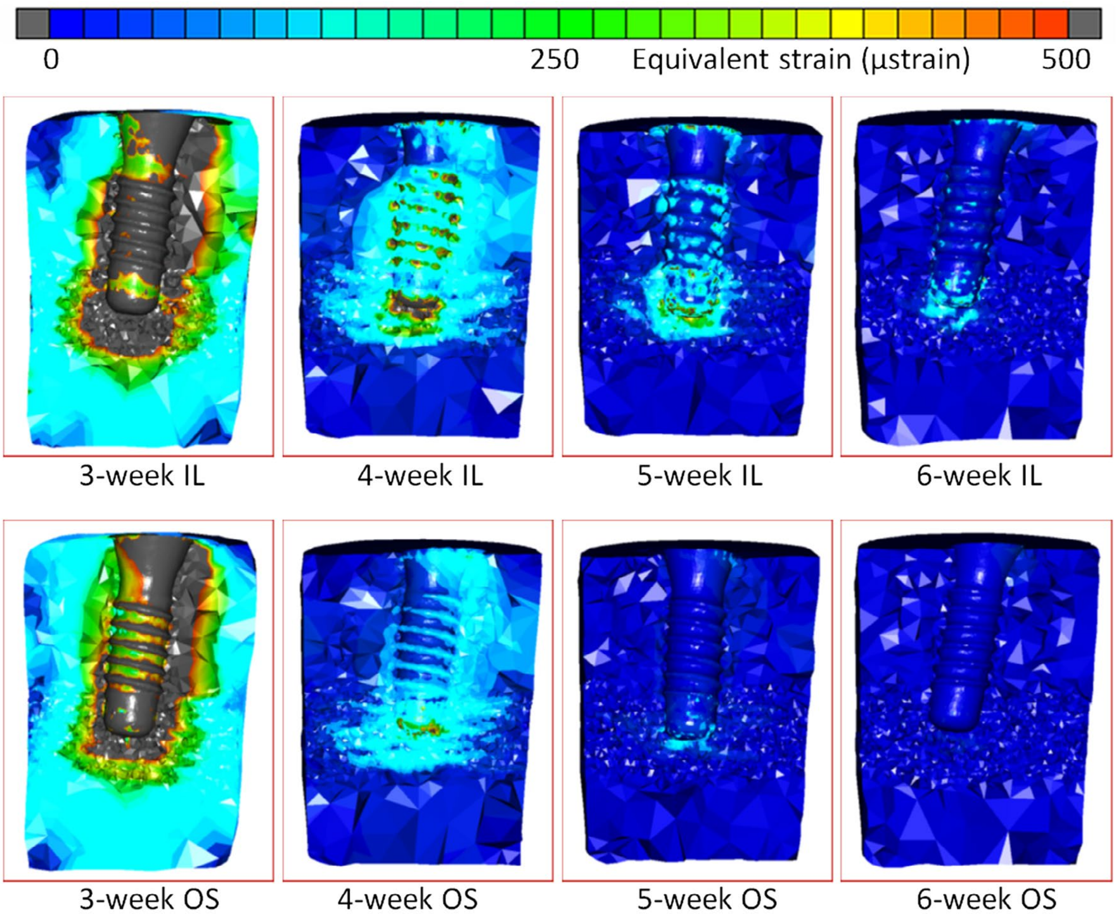

Figure 5. Comparison of the strains in antler tissue.
Notes: From above to below: immediate loading (IL) and osseointegration (OS) models. From left to right, models in 3, 4, 5, 6 weeks.

6 weeks which is similar to that of human cortical bone (14 GPa) usually used in finite element analysis. That was in agreement to the first null hypothesis. This behavior is in agreement with the remodelling process of the bone that is initiated by the insertion of the implant and the activation of the osteoblasts and consequent bone apposition. Moreover, this is consistent with the studies on other animals and humans. Ramachandran et al. (2016) investigated the radiographic changes in bone density associated with immediate implant loading protocols. The mean pixel greyscale values at the lateral apical level showed a steady increase from baseline to three months and from three months to six months. The mean crestal pixel greyscale values showed a decrease from baseline to three months but an increase between three and six months. Mainetti et al. (2015) investigated the sequential healing at immediately loaded implants installed immediately after tooth extraction and found that the bone density increased slightly during the first and second week. Mainetti et al. (2015) observed that bone mineralization was found to be increased at the 1-month observation, while it remained stable.

Due to the increasing material characteristics of the antler tissue during the healing time, the displacements and stresses in implant and strains in antler tissue were reduced in all models. However, opposite behavior was observed with the stresses in antler tissue. The statistical results demonstrated that the differences between different time points were significant ($P < .05$) except among following groups: Displacements in implant between 5-week and 6-week OS models, stresses in implant between 3-week and 4-week IL models and between 5-week and 6-week IL models, stresses in antler tissue between 3-week and 4-week IL models, between 5-week and 6-week IL models, between 3-week and 4-week OS models, and between 5-week and 6-week OS models, strains in antler tissue between 5-week and 6-week IL models and between 5-week and 6-week OS models. Displacements and stresses in implants were decreased and the distributions of stresses in implant were concentrated over small area while the healing time was progressing. The possible reason is that stresses in implant can be more transferred to surrounding antler tissue resulted in decreased displacements and stresses in implants and increased stresses in antler tissue as its BMD and Young's Modulus was increased. When the BMD and Young's modulus of antler tissue increased after 5 weeks and 6 weeks, stresses in the antler tissue were not only concentrated on the tip and threads region, but located on the neck region as well. This results is consistent with a couple of recently published studies (Premnath et al. 2012; Marcián et al. 2014; Sugiura et al. 2015) which concluded that more dense the bone is, the smaller displacements and stresses in implant and stresses in bone. Strains in antler tissue were reduced during the healing time since the deformation of the bone tissue by strain is inversely correlated to its stiffness. The higher the stiffness of the bone, the lower the strain value (Currey 1988). The maximum strains in antler tissue with IL model after 3 weeks reached 9,879 μstrain, but decreased to 2,188 μstrain after 4 weeks and 363 μstrain after 6 weeks.

At the same time point, the biomechanical parameters of the OS model were lower than that of the IL model and the distribution was smaller than that of the IL model. The values had significant differences ($P < .05$) except for the stresses in implant of 3-week models, suggesting that the load bearing capacity of the antler tissue around IL implants was weak compared to fully integrated implants. The results are substantially consistent with the final null hypothesis and many studies. For example, the study of Han et al. (2014) indicated that IL significantly increased bone stress, compared with OS condition. Winter et al. (2013) discovered that changing the contact type between implant and bone from friction free to rigid led to a reduction of implant displacement. On the other hand, reducing the Young's modulus of bone for simulating an immediately loaded implant caused a substantial increase in displacement of the implant.

This study had several limitations. First, material properties of the antler tissue were assumed to be isotropic and linearly elastic. Secondly, an empirical equation was used to calculate Young's modulus of antler tissue from BMD. However, the same conditions were applied to all models. Therefore the results are compatible and valuable.

5. Conclusions

Within the limits of this study, it can be found that the BMD and Young's modulus of the antler tissue around an implant increased during the healing time accompanied by the bone remodelling process. The biomechanical parameters of OS models were significantly lower than that of IL models at each time point. In conclusion, antler tissue showed the same biomechanical properties as human bone in investigating the bone remodelling around implants, therefore the use of sika deer antler as a novel model is promising. Further study is currently under investigation in terms of histological analysis and comparing the bone remodelling of immediately loaded and osseointegrated implants.

Acknowledgements

The authors thank the staff of Raptor Center and Wildlife Parc Hellenthal, especially Mr. Joerg Niesters, Mr. Karl Fischer, Mr. Dirk Wynands and Dr. Martin Boettcher for care of the animals, thank the staff of Endowed Chair of Oral Technology, University of Bonn, Dr. Susanne Reimann and Ms. Anna Weber for preparing and scanning the specimens by μCT scanner, and thank Mr.Tim Klunter for taking out the specimens from antlers.

Disclosure statement

The study sponsors have no involvement in the study design, in the collection, analysis and interpretation of data, in the writing of the manuscript, or in the decision to submit the manuscript for publication.

Funding

This investigation was supported by Friadent GmbH (Mannheim, Germany) and Straumann GmbH (Freiburg, Germany) and the National Natural Science Foundation of China [Grant number 11702231].

References

Albrektsson T, Brånemark PI, Hansson HA, Lindström J. 1981. Osseointegrated titanium implants. Requirements for ensuring a long-lasting, direct bone-to-implant anchorage in man. Acta Orthop Scand. 52:155–170.

Al-Sawai AA, Labib H. 2016. Success of immediate loading implants compared to conventionally-loaded implants: a literature review. J Investig Clin Dent. 7:217–224.

Barndt P, Zhang H, Liu F. 2015. Immediate loading: from biology to biomechanics. Report of the Committee on Research in fixed Prosthodontics of the American Academy of fixed Prosthodontics. J Prosthet Dent. 113:96–107.

Bassi F, Carr AB, Chang TL, Estafanous EW, Garrett NR, Happonen RP, Koka S, Laine J, Osswald M, Reintsema H, et al. 2013. Functional outcomes for clinical evaluation of implant restorations. Int J Prosthodont. 26:411–418.

Beaupré GS, Orr TE, Carter DR. 1990. An approach for time-dependent bone modeling and remodeling–theoretical development. J Orthop Res. 8:651–661.

Boven GC, Raghoebar GM, Vissink A, Meijer HJ. 2015. Improving masticatory performance, bite force, nutritional state and patient's satisfaction with implant overdentures: a systematic review of the literature. J Oral Rehabil. 42:220–233.

Brånemark PI. 1983. Osseointegration and its experimental background. J Prosthet Dent. 50:399–410.

Caulkett N, Haigh JC. 2007. Deer (Cervids). In: West G, Heard D, Caulkett N, editors. Zoo animal and wildlife

immobilization and anaesthesia. Ames Iowa: Blackwell Publishing; p. 607–612.
Chen PY, Stokes AG, McKittrick J. 2009. Comparison of the structure and mechanical properties of bovine femur bone and antler of the North American elk (Cervus elaphus canadensis). Acta Biomater. 5:693–706.
Currey JD. 1988. Strain rate and mineral content in fracture models of bone. Journal of Orthopaedic Research. 6:32–38.
Currey JD, Landete-Castillejos T, Estevez J, Ceacero F, Olguin A, Garcia A, Gallego L. 2009. The mechanical properties of red deer antler bone when used in fighting. J Exp Biol. 212:3985–3993.
De Smet E, Jaecques SV, Wevers M, Jansen JA, Jacobs R, Sloten JV, Naert IE. 2006. Effect of controlled early implant loading on bone healing and bone mass in guinea pigs, as assessed by micro-CT and histology. Eur J Oral Sci. 114:232–242.
Duyck J, Ronold HJ, Van Oosterwyck H, Naert I, Vander Sloten J, Ellingsen JE. 2001. The influence of static and dynamic loading on marginal bone reactions around osseointegrated implants: an animal experimental study. Clin Oral Implants Res. 12:207–218.
Esposito M, Siormpas K, Mitsias M, Bechara S, Trullenque-Eriksson A, Pistilli R. 2016. Immediate, early (6 weeks) and delayed loading (3 months) of single implants: 4-month post-loading from a multicenter pragmatic randomised controlled trial. Eur J Oral Implantol. 9:249–260.
Frost HM. 2004. A 2003 update of bone physiology and Wolff's Law for clinicians. Angle Orthod. 74:3–15.
Gotfredsen K, Berglundh T, Lindhe J. 2002. Bone reactions at implants subjected to experimental peri-implantitis and static load-A study in the dog. J Clin Periodontol. 29:144–151.
Gottlow J, Dard M, Kjellson F, Obrecht M, Sennerby L. 2012. Evaluation of a new titanium-zirconium dental implant: a biomechanical and histological comparative study in the mini pig. Clin Implant Dent Relat Res. 14:538–545.
Granić M, Katanec D, Vučićević Boras V, Sušić M, Jurič IB, Gabrić D. 2015. Implant stability comparison of immediate and delayed maxillary implant placement by use of resonance frequency analysis–a clinical study. Acta Clin Croat. 54:3–8.
Han J, Hou J, Zhou G, Wang C, Fan Y. 2014. A histological and biomechanical study of bone stress and bone remodeling around immediately loaded implants. Sci China Life Sci. 6:618–626.
Huang Y, van Dessel J, Martens W, Lambrichts I, Zhong WJ, Ma GW, Lin D, Liang X, Jacobs R. 2015. Sensory innervation around immediately vs. delayed loaded implants: a pilot study. Int J Oral Sci. 7:49–55.
Kunnekel AT, Dudani MT, Nair CK, Naidu EM, Sivagami G. 2011. Comparison of delayed implant placement vs immediate implant placement using resonance frequency analysis: a pilot study on rabbits. J Oral Implantol. 5:543–548.
Launey ME, Chen PY, McKittrick J, Ritchie RO. 2010. Mechanistic aspects of the fracture toughness of elk antler bone. Acta Biomater. 6:1505–1514.
Lekholm U. 2003. Immediate/early loading of oral implants in compromised patients. Periodontol. 2000(33):194–203.
Mainetti T, Lang NP, Bengazi F, Sbricoli L, Soto Cantero L, Botticelli D. 2015. Immediate loading of implants installed in a healed alveolar bony ridge or immediately after tooth extraction: an experimental study in dogs. Clin Oral Implants Res. 4:435–441.
Marcián P, Borák L, Valášek J, Kaiser J, Florian Z, Wolff J. 2014. Finite element analysis of dental implant loading on atrophic and non-atrophic cancellous and cortical mandibular bone - a feasibility study. J Biomech. 47:3830–3836.
Matin K, Senpuku H, Hanada N, Ozawa H, Ejiri S. 2003. Bone regeneration by recombinant human bone morphogenetic protein-2 around immediate implants: a pilot study in rats. Int J Oral Maxillofac Implants. 2:211–217.
Paramio MAR, Muñoz-Cobo J, Moro J, Gutierrez R, Oya A, Tellado S, Azorit C. 2012. Assessing red deer antler density with a hydrostatic method versus a new parametric volume-modelling technique using 3D-CAD. Anim Prod Sci. 52:750–755.
Premnath K, Sridevi J, Kalavathy N, Nagaranjani P, Sharmila MR. 2012. Evaluation of stress distribution in bone of different densities using different implant designs: a three-dimensional finite element analysis. J Indian Prosthodont Soc. 13:555–559.
Rahimi A, Klein R, Keilig L, Abboud M, Wahl G, Bourauel C. 2009. Development and design of a novel loading device for the investigation of bone adaptation around immediately loaded dental implants using the reindeer antler as implant bed. J Biomech. 42:2415–2418.
Ramachandran A, Singh K, Rao J, Mishra N, Jurel SK, Agrawal KK. 2016. Changes in alveolar bone density around immediate functionally and nonfunctionally loaded implants. J Prosthet Dent. 115:712–717.
Romanos GE, Nentwig GH. 2006. Immediate versus delayed functional loading of implants in the posterior mandible: a 2-year prospective clinical study of 12 consecutive cases. Int J Periodontics Restorative Dent. 26:459–469.
Sato N, Kuwana T, Yamamoto M, Suenaga H, Anada T, Koyama S, Suzuki O, Sasaki K. 2014. Bone response to immediate loading through titanium implants with different surface roughness in rats. Odontology. 7:249–258.
Simion M, Benigni M, Al-Hezaimi K, Kim DM. 2015. Early bone formation adjacent to oxidized and machined implant surfaces: a histologic study. Int J Periodontics Restorative Dent. 1:9–17.
Sugiura T, Yamamoto K, Kawakami M, Horita S, Murakami K, Kirita T. 2015. Influence of bone parameters on peri-implant bone strain distribution in the posterior mandible. Med Oral Patol Oral Cir Bucal. 20:66–73.
Tassani S, Ohman C, Baruffaldi F, Baleani M, Viceconti M. 2011. Volume to density relation in adult human bone tissue. J Biomech. 44:103–108.
Testori T, Del Fabbro M, Galli F, Francetti L, Taschieri S, Weinstein R. 2004. Immediate occlusal loading the same day or the after implant placement: comparison of 2 different time frames in total edentulous lower jaws. J Oral Implantol. 30:307–313.
Torroella-Saura G, Mareque-Bueno J, Cabratosa-Termes J, Hernández-Alfaro F, Ferrés-Padró E, Calvo-Guirado JL. 2015. Effect of implant design in immediate loading. A randomized, controlled, split-mouth, prospective clinical trial. Clin Oral Implants Res. 26:240–244.
Vandamme K, Naert I, Geris L, Sloten JV, Puers R, Duyck J. 2007. Histodynamics of bone tissue formation around

immediately loaded cylindrical implants in the rabbit. Clin Oral Implants Res. 4:471–480.

Webster D, Schulte FA, Lambers FM, Kuhn G, Müller R. 2015. Strain energy density gradients in bone marrow predict osteoblast and osteoclast activity: a finite element study. J Biomech. 48:866–874.

Wiesner H, von Hegel G. 1985. Practical advice concerning the immobilization of wild and zoo animals. Tierarztl Prax. 13:113–127.

Winter W, Klein D, Karl M. 2013. Effect of model parameters on finite element analysis of micromotions in implant dentistry. J Oral Implantol. 39:23–29.

Zuffetti F, Esposito M, Galli F, Capelli M, Grandi G, Testori T. 2016. A 10-year report from a multicentre randomised controlled trial: Immediate non-occlusal versus early loading of dental implants in partially edentulous patients. Eur J Oral Implantol. 9:219–230.

Acknowledgements

First of all I would like to thank my supervisor Professor Christoph Bourauel for his kind assistance, constant support and flexibility right from the beginning till the end of this work. I thank the members of my Ph.D. committee, Professor Friedhelm Heineman, Professor Gerhard Wahl and Professor Helmut Stark. I greatly appreciate their interest and help in my work.

I am grateful to all the supportive colleagues I have met along the way. The staff of Raptor Center and Wildlife Parc Hellenthal, especially Mr. Joerg Niesters, Mr. Karl Fischer, Mr. Dirk Wynands and Dr. Martin Boettcher for care of the animals. Thank Dr. Susanne Reimann and Ms. Anna Weber for preparing and scanning the specimens by μCT scanner, and thank Mr. Tim Klunter for taking out the specimens from antlers. A special thanks to Dr. Keilig for his technical support and knowledge contribution during this work.

I will always be grateful to PD. Dr. Hasan, who supports me in every scientific step I make, guiding me into the field of numerical study and helping me in developing experimental techniques and writing scientific articles.

I would like to express my deepest gratitude to my family who unconditionally support me in all my life and in every decision I take. I believe that this Ph.D. belongs as much to you as it does to me.

Last but not least, I gratefully acknowledge the support from the colleagues of Oral Technology, University of Bonn and the financial support by China Scholarship Council (CSC).